

**REVIEW OF AERONAUTICAL FATIGUE
INVESTIGATIONS IN JAPAN
DURING THE PERIOD JUNE 2013 TO MAY 2015**

Edited by

Nobuo Takeda
The University of Tokyo

Shigeru Machida
Takao Okada
Japan Aerospace Exploration Agency

For Presentation at the 34rd Conference of
the International Committee on Aeronautical Fatigue and Structural Integrity

Helsinki Finland, 1-2 June, 2015

Contents

	page
1. INTRODUCTION	4
2. FATIGUE AND FAILURE IN METALLIC MATERIALS AND COMPONENTS	6
2.1 Effect of Shot Peening on Low Cycle Fatigue Behavior of Ti-6Al-4V	6
2.2 Shot Peening Residual Stress Evaluation from 3D Finite Element Simulation	7
2.3 Closed Form Equations of Stress Intensity Factors for Angle Shaped Cross-section with Through Crack	9
2.4 WFD Evaluation of Riveted Lap Joint	11
2.5 Analytical Modeling of Mechanical Joint for New Monitoring Method	12
3. FATIGUE AND FAILURE IN COMPOSITE MATERIALS AND COMPONENTS	14
3.1 Development of Composite Structural Guide Vane for the New Turbo Fan Engine	14
3.2 Evaluation of Fatigue Properties of Thick CFRP Laminates with Toughened Interlaminar in the Out-Of-Plane and the In-Plane Transverse Directions	16
3.3 Evaluation of Transverse Crack Initiation in Cross-Ply and Quasi-Isotropic CFRP Laminates under Fatigue Loading	18
3.4 Fatigue Strength of Adhesively Bonded Joints of CFRP with Laser Surface Treatment	19
3.5 Evaluation of Failure Mechanisms on Composite Stiffened Panels with a Two-Bay Notch Damage	21
3.6 Experimental Study on Partial Composite Wing Structure	22
4. STRUCTURAL HEALTH MONITORING	24
4.1 Application of Distributed Fiber Optic Strain Sensors for Local Indentation/Impact Damage Detection in Foam Core Composite Sandwich Structures	24
4.2 Development of Optical Fiber Sensor Based Impact Damage Detection System for Composite Airframe Structures	26

4.3 Development of Ultrasonic Based Structural Health Monitoring (SHM) Technology with MFC and FBG Hybrid Sensor System for Aircraft Structures	28
5. LIFE EVALUATION ANALYSIS	29
5.1 Bayesian Approach to Load Enhancement Factor	29
6. FULL SCALE TESTING	31
6.1 XP-1&XC-2 Strength Test/ ATD Strength Test/ Crashworthiness Technology	31
6.2 Curved Panel Fatigue Test for MRJ-200 Pressurized Cabin Structure	32
7. MISCELLANEOUS	33
7.1 An Amphibian and the Concept of Its Derivative Model for Firefighting Application	33
7.2 Development of Test and Analysis Methods for Lightning Strike on CFRP Structures	35
ACKNOWLEDGEMENTS	36
TABLES AND FIGURES	37

1. INTRODUCTION

Nobuo Takeda, National Delegate, The University of Tokyo

This review summarizes the papers on the study of aeronautical fatigue, structural integrity and related themes conducted in Japan during June 2013 to May 2015.

The papers were contributed by following organizations:

Japan Aerospace Exploration Agency (JAXA)
Technical Research and Development Institute (TRDI), MOD
SOKEIZAI Center
Mitsubishi Heavy Industries, Ltd. (MHI)
Mitsubishi Aircraft Corporation
Kawasaki Heavy Industries, Ltd. (KHI)
Fuji Heavy Industries, Ltd. (FHI)
IHI Corporations
IHI Aerospace Co., Ltd.
ShinMaywa Industries, Ltd.
Toray Industries, Inc.
The University of Tokyo
Kyushu Institute of Technology
Tokyo Metropolitan University
Waseda University

The general activities on aircraft development program in Japan during 2013 to 2015 is summarized as follows:

- The development of MRJ (Mitsubishi Regional Jet, 70- to 90-seat regional jets) aircraft is in the final stage. The maiden flight is expected late in 2015. The production is underway at Mitsubishi Aircraft Corporation in Nagoya. Curved Panel Fatigue Tests for MRJ-200 Pressurized Cabin Structure have been successfully conducted to evaluate the widespread fatigue damage.
- Since 2001, TRDI has been conducting a simultaneous development of the next-generation maritime patrol aircraft (XP-1) which is the successor to P-3C operated by Japan Maritime Self-Defense Force and the next-generation cargo aircraft (XC-2) which is the successor to C-1 etc. operated

by Japan Air Self-Defense Force. The development of XP-1 has successfully completed in March, 2013. The structural integrity of XP-1 was finally verified by three full scale strength tests (static, durability and damage tolerance). In the development of XC-2 the strength test has been continued to verify the strength of XC-2 airframe.

- The second phase of “Civil Aviation Fundamental Technology Program - Advanced Materials & Process Development for Next-Generation Aircraft Structures” (FY2003-2015) have been conducted at the SOKEIZAI Center, in collaboration with industries, universities and national laboratories. The program includes two projects on (1) Composite Structure Health Monitoring and Diagnosis, and (2) Material Development and Processing of Next-Generation Titanium Alloy Structural Members.

2. FATIGUE AND FAILURE IN METALLIC MATERIALS AND COMPONENTS

2.1 Effect of Shot Peening on Low Cycle Fatigue Behavior of Ti-6Al-4V

Hiroshi Nakamura^{1*}, Tatsuhito Honda¹, Joris Prou², Mitsuyoshi Tsunori²

¹ *IHI Corporation, Aero-Engine & Space Operations*

² *IHI Corporation, Research laboratory*

Ti-6Al-4V has been used for rotating components of aero engine low temperature sections such as disks and blades because of its excellent specific strength and fatigue capability. Rotating turbine components are routinely subjected to cyclic thermal stress, body force and pressure. This situation causes low cycle fatigue (LCF) damage during operation. It is important to improve LCF capability because structural safety and integrity of turbine components are dominated by fatigue failure. Shot peening is a surface enhancement technique that causes compressive residual stress in the material surface layer and improve fatigue life. Several studies have reported shot peening effect on high cycle fatigue properties, however, only a few studies deal with LCF capability. This study investigates shot peening effect on LCF behavior of Ti-6Al-4V. Two types of specimens were used in this study. One is polished plate specimen. Another is plate with hole which is simulated actual features such as bolt hole of turbine disk. Shot peening was conducted to both types of specimens after machined. Fatigue tests were carried out using as machined specimen and shot peened specimen. An X-ray diffraction method was used to measure residual stresses on the specimen surfaces. Crack propagation analyses were conducted to assess LCF life of shot peened specimen.

Compressive residual stress layer was observed in the surface of polished plate specimen and peened specimen (Fig.1(a)). Peened plate surface indicated higher and deeper compressive residual stress than that of as machined. Average LCF life of peened plate specimen was longer than that of as machined (Fig.2(a)). This result suggests that LCF capability of peened plate specimen was enhanced due to higher compressive residual stress. Variability of LCF life of peened plate specimen was similar to that of machined specimen. Both polishing and peening were conducted under controlled conditions, this may result in stable compressive residual stress layer in the surface. As a result, variability of LCF life was similar between peened plate specimen and as

polished specimen. As machined hole specimen and shot peened hole specimen showed similar compressive residual stress distribution (Fig.1(b)). Peened hole specimen indicated almost same average LCF life as that of as machined hole, whereas smaller variability of LCF life were observed in peened hole specimen (Fig.2(b)). This may be attributed to more stable compressive residual stress caused by shot peening than that of as machined hole in actual features.

Average LCF life of polished plate was enhanced by shot peening. This effect was assessed in view of fatigue crack propagation analyses including to the compressive residual stress. Simple assumption in this investigation is that shot peened specimen and as machined specimen are same crack initiation lives. Crack initiation lives were estimated based on the crack propagation analyses using LCF test results of as machined specimen. Predicted life used initial residual stress distribution was longer than experimental results. Previous study showed that residual stress relaxation was observed during LCF tests [1]. Thus, residual stress relaxation was considered if the applied stress to the LCF specimen is larger than material yield stress. As a result, LCF life can be predicted within a factor of 4 scatter band (Fig.3). This scatter agrees with variability of LCF test results.

Aknowlegement

This study was conducted under the collaborative investigation with Japan Aerospace Exploration Agency (JAXA) as a part of “Advanced Fan Jet Research(aFJR)” project.

Reference

- 1) H. Nakamura, M. Takanashi, Y. Itabashi, H. Kuroki and Y. Ueda, Proceedings of ASME Turbo Expo 2011, GT2011-46847.

2.2 Shot Peening Residual Stress Evaluation from 3D Finite Element Simulation

Joris Prou¹, Mitsuyoshi Tsunori¹ and Hiroshi Nakamura²

¹ *IHI Corporation, Structural Strength Department*

² *IHI Corporation, Engine Technology Department*

Shot peening is a surface enhancement process used to improve component fatigue life by impacting hard shots at high velocity on the target material. This process induces a surface compressive residual stress layer that is recognized to improve the fatigue resistance. By including the shot peening benefits in the design phase, it is expected that jet engine components such as disks can be lighten without impairing their fatigue resistance. However, to take full advantage of the shot peening process, the effect of the peening conditions and the work piece geometry on the residual stress distribution need to be quantitatively assessed. Performed on a purely experimental basis, such investigations turn out to be costly and time consuming. The use of finite element simulation is thus a promising alternative to reach optimal peening conditions. With the improvement of computational power, shot peening simulation models switched from axisymmetric models [1] to the more realistic multiple impact three dimensional models [2], where effects due to inclined shots and peening coverage (percentage of work piece surface impacted) can be taken into account [3]. In the latter case, simulated residual stress distributions are usually found to be in good agreement residual stress measurement.

This presentation will address the effect on the residual stress distribution of the peening conditions including shot size, velocity and impingement angle, and the effect of the target specimen geometry such as flat surface, edge or hole features. The study was conducted from single shot and multiple shots simulations based on three dimensional finite element analyses. The finite element models for the different target geometries are shown in Fig. 4. In both single and multiple shots cases, the shot impact simulations were performed using a dynamic analysis procedure with ABAQUS/Explicit. Ti-6Al-4V was selected as the target material for this study since its strength-to-weight ratio and good corrosion resistance make it one of the major alloys used in aerospace engine components. Target material was modeled as elastoplastic, while the shots as spherical rigid surfaces. In the multiple shots analyses, the shot impact positions were randomly distributed over a target region on the work piece surface, similarly to the procedure described in [2]. The required number of shot was determined to replicate the peening process full coverage (98%) based on the amount of plastic strain for the element at the work piece surface. In the single shot analysis the in-depth residual stress profiles were estimated directly below the shot

impact location, while for multiple shots analysis the residual stresses distributions were estimated by an averaging procedure.

Based on the finite element simulations briefly described above, residual stress distribution could be evaluated and the effect of the peening process conditions and work piece geometry could be discussed. While shot velocity and impingement angle showed a large influence on both the maximum compressive residual stress and compressive layer thickness, the shot size affects primarily the compressive layer thickness, which was found to vary linearly with the shot size (Fig. 5). Furthermore, simulation results indicated that at the vicinity of edge or hole features there exist a region with a characteristic size of the shot diameter order where the magnitude of the residual stress is decreased (Fig. 6).

Aknowlegement

This study was conducted under the collaborative investigation with Japan Aerospace Exploration Agency (JAXA) as a part of “Advanced Fan Jet Research(aFJR)” project.

References

- [1] E. Rouhaud, A. Oakka, C. Ould, J.L. Chaboche, M. Francois, Finite Elements Model of Shot Peening, Effects of Constitutive Laws of the Material. Proceedings of the 9th International Conference on Shot Peening, 2005, pp. 107-112 .
- [2] H. Miao, S. Larose, C. Perron M. Levesque, On the potential applications of a 3D random finite element model for the simulation of shot peening. Advances in Engineering Software, 2009, 40[10], pp. 1023-1038.
- [3] V. Schulze, M. Klemenz, M. Zimmermann, State of the Art in Shot Peening Simulation. Proceedings of the 10th International Conference on Shot Peening, 2008, pp. 53 – 62

2.3 Closed Form Equations of Stress Intensity Factors for Angle Shaped Cross-section with Through Crack

Toshimi Taki*

Kawasaki Heavy Industries, Ltd.

Structural parts with angle shaped cross-section are commonly used in aircraft primary structures. The examples of such parts are spar chords of wing, stringers of wing skin, chords of fuselage frame, etc. Damage tolerance analysis is required for principal structural elements and the angle section parts are often classified as principal structural elements. Calculation of stress intensity factors (SIF's) is necessary in the damage tolerance analysis assuming initial cracks in the parts. For angle section parts, initial cracks are usually assumed at the edge of the fastener holes in the parts. Unfortunately, SIF's of such crack configurations are not published in the handbooks of SIF's or research papers. SIF models of angle section parts are not included in AFGROW and NASGRO, too. A simplified approach for the SIF calculation, which assumes a strip with equivalent width to the angle section, has been commonly used in the aircraft industries. Usually, the width of the equivalent strip is set to the sum of the widths of the both legs. But the accuracy of the approach is not evaluated. This means that finite element analysis is the only method to calculate accurate SIF's of angle section parts. In practical stand point, closed form equations are convenient for some purposes such as parametric study of the crack growth analysis. Closed form equations for angle section parts are expected to be developed and the accuracy of the equations should be evaluated.

SIF's of angle section parts with initial cracks at the edge of fastener holes can be calculated by "similarity method" or "compounding method", if SIF solutions of various configurations of angle section parts with through cracks are available. The purpose of this paper is to develop closed form equations of SIF's for angle section parts with through cracks under uniform tension load. In this study, two crack configurations, (1) through crack from free edge, and (2) internal through crack in one leg were considered (Fig.7). Various angle section configurations were considered in the study, equal leg widths with equal or different thicknesses, different leg widths with equal or different thicknesses.

Finite element analysis (MSC-NASTRAN) was used for the analysis of SIF's in the study. Plate elements with membrane and bending stiffness, CQUAD4 and CTRIA3, were used to model the angle with through crack (Fig.8). Total energy method and virtual crack closure technique were applied for the calculation of SIF's from the output of NASTRAN analysis. Same SIF values were obtained with the both methods. Closed

form equations of SIF's for the angle configurations described above were developed and the accuracy of the equations was evaluated. The errors of the equations are 2% to 4%. For through crack from free edge, the effect of thickness to SIF is significant when the crack approaches another leg (Fig.9). For internal crack in one leg, strip model with the width of one leg is applicable. The results mean that the stiffening effect of another leg is small. It is shown that the simplified approach commonly used in the aircraft industries is not accurate or conservative. The closed form equations developed in the study are more accurate and should be used.

2.4 WFD Evaluation of Riveted Lap Joint

Takao Okada¹, Min Liao², Shigeru Machida¹, Gang Li², Guillaume Renaud²

¹*Japan Aerospace Exploration Agency*

²*National Research Council Canada*

The limit of validity (LOV) is a new airworthiness requirement (14 CFR Parts 25, 26, 121) for some airplanes, which includes both safe life and damage tolerant philosophies. The damage tolerant philosophy prevents abrupt structural failure by a maintenance program based on engineering data using initial cracks and crack growth behavior during operation. The fatigue life between an initial crack to a crack of a certain length needs to be predicted reasonably well. Many research activities for damage tolerant evaluation have been conducted for many years and there are many tools to evaluate crack growth behavior. The range of this research is between coupons and full scale components. On the other hand, the LOV is the period of time (in load cycles, flight hours, or both), up to which it has been demonstrated that widespread fatigue damage (WFD) is unlikely to occur in an airplane structure by virtue of its inherent design characteristics and maintenance actions. The WFD involves simultaneous presence of multiple cracks at multiple locations that are of sufficient sizes and density such that the structure will no longer meet the residual strength requirement. Some WFD cracks are hidden in the structure and very difficult to detect. As such the WFD evaluation usually does not assume the same initial crack size as the damage tolerant evaluation. The fatigue life from the first operation day to a crack growing to a certain length is required for the WFD evaluation. Comparing to the damage tolerant analysis, the WFD evaluation method is not well known and not well established yet. Because of this

situation, research on WFD assessment for gaining knowledge of WFD, and research on WFD evaluation by experiments and analysis are imperative for aircraft OEM and some operators in order to comply with the new airworthiness requirement.

In this paper, a riveted lap joint flat panel is used for evaluating the early stage of WFD development, i.e., WFD onset. The riveted joint is a single lap joint with 3 rows of 20 fasteners, and a narrow plate is attached to the middle row to simulate a fuselage panel stringer. Nine button head rivets are used on both sides of the panel while countersunk rivets are used at the other locations. Constant amplitude fatigue load is applied to the lap joint panel, and strain data are obtained in order to evaluate the strain distribution around the fasteners. Visual inspection around each fastener using a CCD camera is conducted during the fatigue test to detect locations and lengths of the cracks formed and propagating from the rivet holes. In most cases, the locations of the cracks are above the horizontal centerline of the rivet holes, and apparent fretting damage is observed near the crack nucleation area on the faying surface of the joint and around the fastener holes (Figure 10). Numerical analysis of the riveted lap joint is also conducted using 3D global-local finite element (FE) modeling to predict the strain distribution during the manufacturing of the lap joint and then during the fatigue loading (Figure 11). Strain data measured from the test is used for validating the FE analysis. The effects of the riveting squeezing force and clearance fit on the joint stress/strain condition and then on the fatigue life assessment are studied in this paper. The cycles for a crack to 0.5-mm is predicted using the Smith-Watson-Topper (SWT) equation. The geometry correction factor and residual stress correction factor for crack growth analysis are evaluated using AFGROW and a NRC in-house tool, CanGROW. CanGROW is also used to evaluate EIFS distribution calculation and life distribution up to the cycles to the first linkup. The analytical models and results are compared with the test data to improve the knowledge of the WFD feature and to improve research efficiency by reducing test quantity and cost.

2.5 Analytical Modeling of Mechanical Joint for New Monitoring Method

Shigeru Machida

Japan Aerospace Exploration Agency

Historically, structural damping values are determined based on data of experiments or existing aircrafts which have similar structural layout and same materials. For a new aircraft which has new materials and unique structural layout, it is necessary to establish a method to estimate structural damping characteristics. Regarding a fatigue evaluation of aircraft structures, “mechanical joint” is one of the susceptible areas to be designed carefully for preventing catastrophic failure, such as widespread fatigue damage. However, an inspection method for widespread fatigue damage is not established yet. In order to reduce structural risk, a proactive, rather than reactive, approach should be adopted such as structural monitoring during all life of aircraft. In a previous paper ¹⁾, a new method for characterizing degradation and damages inside a mechanical joint from the information of structural damping, a non-linear response against cyclic loading, was presented as an unique monitoring concept for structural joints. Addition to that, the new analytical model which can express structural damping characteristics of riveted lap joints was proposed.

The term of “Structural Damping” means the energy dissipation properties of structure and it is well known that interfacial slip phenomena at structural joints are the primary source of “Structural Damping”, which may be affected by types of joint and conditions of faying surfaces. Therefore, it was strongly expected that structural damping properties can show an important information of conditions in faying such as fretting wear, corrosion and cracking. Several riveted lap joint specimens were tested under constant cyclic loading. Specimens can represent the part of circumferential single lap joint which has typical three rivet rows, Fig. 12. The cyclic load tests were conducted under load control using a constant amplitude sinusoidal waveform. Stopping cyclic loading at specific cycles, an extensometer was installed at the side edge of specimen to measure deflection between two points over the rivet joint under loading. The test results, Fig. 13, showed the unique relationship between energy dissipation per cycle and number of cycles qualitatively.

An analytical joint model was studied by Metherell and Diller²⁾ who investigated an energy dissipation of single lap joint. Their works gave equations which can express a shape of load-deflection hysteresis loop and energy dissipation per cycle under uniform clamping pressure. However the equations could not consider joint stiffness and a load transfer of stick portion. In order to establish governing equations for single lap joint with rivets which has stick part and slip part to transfer loads, the stiffness of stick

portion, K_{ST} , was introduced. The new equations for the displacement as the function of tensile load were established as a new analytical model for rivet joints. Using the results from finite element analyses, Fig. 14, and the load-deflection hysteresis loops from cyclic loading tests with additional specimens, it is shown that the coefficients of the new analysis model can be used for characterizing degradation inside mechanical joints.

The following conclusions can be drawn from present study.

By using the proposed mathematical joint model and improved analysis method, it is possible to quantify the non-linearity of force/displacement hysteresis loop and to identify the coefficients which can explain condition on the faying surface of shear lap joint. Experimental results of join specimens using round-head rivets indicate that the unique relationship between D and number of cycles N and the trend can be explained in four phases as the previous investigation with countersunk rivet specimens. In comparison with the results of countersunk rivet specimens, the range of changing of energy dissipation value is relatively small.

References

- 1) Shigeru Machida, Shuji Kishishita, Yuya Ito, Takao Okada, Motoo Asakawa, New Monitoring Method for Mechanical Joint Using Structural Damping Properties, Proceedings of The 27th Symposium of The International Committee on Aeronautical Fatigue and Structural Integrity, Vol. 2, June 2013, pp. 797-807
- 2) A. F. Metherell, S. V. Diller, Instantaneous Energy Dissipation Rate in a lap Joint – Uniform Clamping Pressure, Journal of Applied Mechanics, Vol. 35, March 1968, pp. 123-128

3. FATIGUE AND FAILURE IN COMPOSITE MATERIALS AND COMPONENTS

3.1 Development of Composite Structural Guide Vane for the New Turbo Fan Engine

Takaomi Inada¹, Hiroyuki Yagi¹, Hideo Morita¹, Rintarou Kajiwara¹, Takehisa Yamada¹, Tsutomu Murakami¹, Koji Miyazawa¹, Takehiko Uchiyama¹, Katsuyoshi Moriya¹, Shinichi Tanaka²

¹*IHI Corporation*

²*IHI Aerospace Co., Ltd.*

Fan exit guide vanes (FEGVs) in turbo fan engines are located just after the fan blades and have a role to remove the swirl from the flow coming from the fan blades to reduce drag and improve efficiency. In recent high bypass ratio engines, the fan exit guide vanes are designed to fulfill aerodynamic requirements, such as low pressure loss, as well as the structural requirement to withstand the engine loads in all operating conditions for weight reduction. Such FEGVs are called as structural guide vanes (SGVs). To improve fuel efficiency of such high bypass ratio engines, fan diameter is tend to increase more and more. The benefits of this trend are however counteracted by the resulting weight increase that cause higher fuel consumption. To achieve higher total fuel efficiency, the structural guide vanes also have to be designed to reduce total weight of the engines. Therefore, composite SGVs are one of the best solutions in terms of structural requirements as well as weight requirements.

This paper describes a development activity of composite structural guide vane using an in-house carbon fiber/thermoplastic resin prepreg and die mold process. So called “a building block approach” was applied for the development (Fig.15). In order to achieve high impact resistance capability against foreign object impact, such as bird strike event, in-house prepreg was developed and evaluated through soft body impact tests. In parallel to material (prepreg) development and evaluation, joint structure between a composite vane and metal parts was developed since SGVs are installed between a fan case and a core of a turbo fan engine and need metal attachment. Flat panel tests were conducted for the joint structure evaluation by applying bending moment to the end which is opposite side to the fixed end. Static loading capability as well as fatigue loading capability was assessed through the tests, and a mechanical joint with adhesive was developed finally. As a next step of building block approach, sub-component tests using a full-size single SGV were conducted. In order to assess load bearing capability as a single vane, a special loading test apparatus and procedure was newly developed. The single vane was fixed to a metal block, which is simulated core structure of an engine, and three axial loads were applied to the top block. The actuation load was controlled to simulate actual engine load as much as possible with some amplification factor. Static loading test followed by fatigue loading test and additional static loading

test was conducted in each vane test. The tested vane was inspected by X-ray CT to assess integrity after the test. As a result, it was confirmed that the developed SGV had sufficient load bearing capability under the design load. Impact bearing capability against soft body / hail ball was confirmed as well. As a final step of the building block, a full-ring component, SGVs assembled with fan case and core structure, was prepared and subjected to static Fan Blade Off (FBO) loading test and fatigue loading test (Fig.16). The test was also successfully completed and demonstrated sufficient capability against FBO requirement.

The SGV development using a building block approach was successfully completed and the SGVs will be applied to a new turbo fan engine soon.

3.2 Evaluation of Fatigue Properties of Thick CFRP Laminates with Toughened Interlaminar in the Out-Of-Plane and the In-Plane Transverse Directions

Atsushi Hosoi^{1*}, Shigeyoshi Sakuma¹, Sen Seki¹, Yuzo Fujita², Ichiro Taketa²,
Hiroyuki Kawada¹

¹*Waseda University*

²*Toray Industries, Inc.*

Bending force is applied due to flexural deformation and inner pressure of fuel at the curved beam in aircraft wing spars made of carbon fiber reinforced plastic (CFRP) laminates. When the bending force is applied at the curved beam, the tensile stress in the out-of-plane direction of the laminates occurs at the curved part. In addition, the latest airplane is made of CFRP laminates with toughened interlaminar. Therefore, it is necessary to evaluate the mechanical properties of CFRP laminates in not only the in-plane direction but also the out-of-plane direction because these properties will be different due to the effect of the toughened interlaminar. First, the test method was verified to conduct static tensile tests and fatigue tests of thick CFRP laminates in the out-of-plane direction. Then, the fatigue properties of thick CFRP laminates with toughened interlaminar were evaluated in both the out-of-plane and the in-plane transverse directions.

Specimens were formed with T800S/3900-2B prepreg. The spool specimens were machined from the thick mother plates which were laminated the preregs

unidirectionally as shown in Fig. 17. The number of lamina in the specimen was 88 for evaluating the mechanical properties in the out-of-plane direction and it was 160 for that in the in-plane transverse direction. The metal tabs were bonded on the top and bottom surfaces. The static tensile tests were performed under displacement control at a tensile speed of 0.1 mm/min. The fatigue tests were performed under load control at stress ratio of $R = 0.1$ and a test frequency of $f = 5$ Hz.

Table 1 shows the mechanical properties of the thick CFRP laminates with toughened interlaminar in the out-of-plane and the in-plane transverse directions. The failure stress is calculated with an applied force per the minimum cross-sectional area in the specimen. It is cleared that the failure stress and strain of the specimens in the out-of-plane direction were 25% and 20% lower than those in the in-plane transverse direction, respectively. Figure 18 shows the S-N curves of the specimens in the out-of-plane and the in-plane transverse directions. It is found that the fatigue life of the specimen in the out-of-plane direction was shorter than that in the in-plane transverse direction from Fig. 18(a). However, the fatigue life can be evaluated equivalently by normalizing with the tensile strength as shown in Fig. 18(b). Therefore, it is thought that the difference of the fatigue strength depends on the difference of the tensile strength. The fracture surfaces were observed by scanning electron microscopy after the static tensile tests and the fatigue tests. The cohesive failure in a fiber layer was observed on the fracture surface after static tensile tests. On the other hand, the interfacial failure between fiber and matrix resin at an edge in a fiber layer was observed on the fracture surface after fatigue test.

The test method was successfully verified for static tensile tests and fatigue tests of the thick CFRP laminates in this study. The tensile strength and fatigue strength of the specimen in the in-plane transverse direction were higher than those of the specimen in the out-of-plane direction due to the effect of toughened interlaminar. It is thought that the difference of the fatigue life in the laminate direction depends on the difference of the tensile strength because the fatigue life can be evaluated equivalently by normalizing with the tensile strength.

3.3 Evaluation of Transverse Crack Initiation in Cross-Ply and Quasi-Isotropic CFRP Laminates under Fatigue Loading

Atsushi Hosoi^{1*}, Yuzo Fujita², Hiroyuki Kawada¹

¹*Waseda University*

²*Toray Industries, Inc.*

A method has been proposed to predict the fatigue life to the transverse crack initiation in cross-ply and quasi-isotropic carbon fiber reinforced plastic (CFRP) laminates in this study. CFRPs have been used as a primary structural members of a commercial airplane, and B787 has realized 20 % reduction in fuel consumption in comparison with a conventional airplane. The ultimate design strain level in aircraft is kept low, approximately 4000-5000 $\mu\epsilon$. At this strain level, the composite materials can withstand large numbers of fatigue cycles without failing, and damage growth is therefore not seen to be a major problem. However, to use composite structures to their full potential and to reduce aircraft weight, design strain levels will need to increase and a partial growth criterion needs to be adopted. When the CFRP laminates are subjected to tensile fatigue loading, transverse cracks are generally first damage in the CFRP laminates and then induce more serious damage, such as delamination or fiber breakage. Therefore, the initiation of a transverse crack in cross-ply and quasi-isotropic CFRP laminates under fatigue loading has been evaluated.

In this study, six kinds of the laminates were formed of the two kinds of the prepregs, T800S/3900-2B with interlaminar toughed layers and T800H/3631 without interlaminar toughed layers. The fiber volume fraction of the prepregs is 56% and 57%, respectively. The cure temperature is 453 K for both prepregs. The unidirectional and the cross-ply laminates of the stacking sequence of $[90]_{12}$, $[0/90_4]_s$ and $[0/90_6]_s$ were formed of the T800S/3900-2B prepreg, and the cross-ply and quasi-isotropic laminates of stacking sequence of $[0/90_2]_s$, $[0/90_6]_s$ and $[45/0/-45/90]_s$ were formed of the T800H/3631 prepreg. Tensile fatigue tests were performed under load control using a hydraulic fatigue testing machine. All tests were run at a stress ratio of $R = 0.1$ and the frequency of $f = 5$ or 100 Hz. Fatigue tests were interrupted at arbitrary loading cycles to observe damage in cross-ply CFRP laminates. The transverse cracks caused in the laminates were observed by optical microscopy and soft X-ray photography.

The transverse crack initiation in the laminates under fatigue loading was evaluated by modifying the Smith-Watson-Topper (SWT) model, which can evaluate the effect of the stress ratio on the fatigue life. Even if the mechanical stress of $R = 0.1$ was applied to the laminates, the stress ratio applied in each lamina in the laminates was varied depending on the applied stress level because of the residual thermal stress. Therefore, it is necessary to consider the effect of the stress ratio. In addition, the size effect should be considered because the transverse crack initiation is affected by the laminate thickness and configuration. Figures 19 and 20 show the evaluation results of the modified SWT model for the fatigue life to the transverse crack initiation of the laminates formed of T800S/3900-2B and T800H/3631, respectively. In the figures, σ_{\max} , σ_a , σ_{ti} show the maximum stress, the stress amplitude and the strength of transverse crack initiation under static tensile loading. The superscript, (90), indicates the stress of 90° layer in the laminates. The fatigue life to the transverse crack initiation can be evaluated with a curve. From the results shown in Fig. 19, it is found that the initiation of the transverse crack in cross-ply laminates can be predicted from the S-N diagram of the unidirectional laminates in 90° direction. On the other hand, from the results shown in Fig. 20, it is found that the initiation of the transverse crack can be predicted for the quasi-isotropic laminates having the edge cracks caused by the free edge effect using the proposed model. The transverse crack initiation in $[45/0/-45/90]_S$ laminates was not observed up to 2×10^8 cycles under the lowest loading condition within this study.

3.4 Fatigue Strength of Adhesively Bonded Joints of CFRP with Laser Surface Treatment

Tomohiro Yokozeki*

The University of Tokyo

Light-weight and high-performance structures are required for aerospace system, and application of carbon fiber-reinforced plastics (CFRP) to the primary structures is expanding. As the large scale structures need assembly of some structural members, highly reliable technology for the joining of CFRP/CFRP and CFRP/metal parts should be established to achieve the light-weight structures. When CFRPs are used for light-weight structural members, adhesive bonding is one of the effective joining methods by consideration of mechanical characteristics and manufacturing process of CFRPs. It is

necessary to develop a powerful method to realize both the high reliability and the efficient process of adhesive bonding.

Adhesive bonding process of CFRPs generally comprises surface polishing (i.e. manual sanding using abrasive papers or treatment by sand blasting), surface cleaning (chemical coating is applied, if necessary), application of adhesives or adhesive films, and curing of adhesives. During this adhesive bonding process, quality stability and rapid process are required for the surface pre-treatment. Development of a reliable and efficient surface pre-treatment process of CFRPs will result in realization of light-weight structures.

Various types of surface treatment are now available: mechanical treatment by abrasive papers and sand blasting, use of peel ply, plasma treatment, various chemical treatments etc. This study investigates the applicability of pulsed CO₂ laser treatment to surface treatment of CFRPs prior to adhesive bonding (Fig.21). Pulsed laser treatment is applied to CFRP surfaces and easy of automation, and thus, is expected to contribute to the development of useful surface pre-treatment process of CFRPs by making the process more stable, faster, and cleaner. In the present study, several laser treatments are applied to CFRPs, and the surface conditions of treated CFRPs are analyzed. Adhesive films are applied to treated CFRPs, and adhesively bonded specimens are prepared and subjected to evaluation of adhesive strength and fatigue strength. Applicability of laser pre-treatment to CFRP bonded structures is investigated by comparison with conventional mechanical surface pre-treatment.

The CFRP samples were fabricated using unidirectional T800S/2592 prepregs (supplied by Toray). Cross-plyed layups were utilized and the stacked materials were cured at 130 °C in the autoclave. It is noted that release agent and release films were used during the manufacturing of CFRPs. Several laser parameters were applied to surface pre-treatment of CFRP and the treated surfaces were analyzed by Laser microscopy (Fig.22), FT-IR, and XPS. For comparison, untreated CFRPs and CFRPs treated by abrasive paper were also analyzed. Based on these experiments, it was found that laser pre-treatment can remove the remained fluerine and silicon, and makes the surface condition of CFRPs similar to that by abrasive paper, if suitable parameters were chosen for laser pre-treatment. Adhesive lap shear strength and fatigue strength were also evaluated (Fig. 23). The results indicated that laser pre-treatment gives

surface conditions similar to abrasive paper in terms of lap shear strength. It is concluded that pulsed laser treatment is applicable to surface pre-treatment of CFRPs.

The present paper investigated the applicability of pulsed CO₂ laser treatment to the surface pre-treatment of CFRPs for adhesively bonded structures. It was demonstrated that suitable laser condition gave surface conditions and adhesive strength similar to the conventional treatment by abrasive paper. The experimental results suggested the usefulness of laser treatment for the bonding process. Laser treatment is a clean process, and possibly makes the pre-treatment process more stable and faster. Further studies on the applicability of this process to other combinations of CFRP and adhesives and dissimilar bonded joints are encouraged.

3.5 Evaluation of Failure Mechanisms on Composite Stiffened Panels with a Two-Bay Notch Damage

Yuichiro Aoki, Shin-ichi Takeda and Yutaka Iwahori

Japan Aerospace Exploration Agency,

Failure mechanisms on composite stiffened panels with a two-bay notch damage is evaluated by both tests and analysis. The two-bay crack was introduced to the panel with three hat-shaped stringers by an artificial engine fragment penetration test. The panels are fabricated by two different fabrication methods, autoclave and VaRTM processes. The panel size is 900 mm long x 750 mm width with a skin thickness of 2 mm. The titanium projectile is designed to simulate an uncontained engine fragment and gives a severe penetration damage in the center of the panel. The total mass of the projectile is 195 g and target velocity is 200m/sec. Non-destructive testing was performed to investigate the damage characteristics in the notched panel as shown in Fig. 24. Then, residual tensile strength test was conducted to verify the damage-tolerance capability of the notched panel. The damage mechanism was examined by a progressive failure analysis based on Hashin's failure criteria and cohesive zone model as shown in Fig. 25. The effect of delamination on the two-bay notch damage growth and failure load of the panel are investigated. The results reveal that typical damage growth path is characterized by fiber breakage perpendicular to the crack tips to be followed by skin and stringer interface damages. The present numerical model has a

potential to simulate the two-bay notch damage growth and to predict the residual strength for the composite panel with a large notch damage.

3.6 Experimental Study on Partial Composite Wing Structure

Hikaru Hoshi¹, Takao Okada¹, Yutaka Iwahori¹, Satoshi Morooka², Naoyuki Watanabe²

¹*Japan Aerospace Exploration Agency*

²*Department of Aerospace Engineering, Tokyo Metropolitan University*

<Framework of research>

Tokyo Metropolitan University (TMU) and Japan Aerospace Exploration Agency are investigating advanced composite structures and smart technology for the next generation aircraft. This project aims to educate the Asian students, and research on advanced aircraft technology. Manufacturing and structural test of the partial composite wing program is major topic of our research project. This partial composite wing program includes demonstration of materials, manufacturing technologies, and measurement techniques.

<Conceptual aircraft>

A composite wing structure was designed to demonstrate the novel technology for the next generation single aisle transport aircraft. Our research target is assumed 150 seat class airliner which is same as the Boeing B737, and the Airbus A320. This conceptual aircraft is shown in figure 26. State of art materials and low cost / high speed manufacturing process are key technology to develop the next generation single aisle aircraft. New stitch composite with Vacuum assisted Resin Transfer Molding (VaRTM) Process was prepared to meet this demand. Stitch composite has high impact resistance characteristics which derive from binding effect of thickness direction stitch thread. Therefore, VaRTM stitch composite was applied to the wing spar to eliminate the in-flight impact problem, complex shape drape problem, and also cost. Spar splice is necessary for easy handling in wing assembly process. Electrical Heating Press Forming (EHPF) method was applied to titanium fitting of spar splice. This EHPF process is able to reduce the machining time and material cost due to near net shape forming.

<Partial composite wing structure>

PCWS is preparing the full scale bending test to evaluate the design strength and the deformation characteristics. The root end of PCWS is installed tension fitting to transfer the bending load between wing structure and loading jig. The region of tension pads is reinforced by CFRP pad-up plate to prevent the un-matured failure before the design ultimate load. The design air load distribution is simplified by many whiffle tree fixtures with 8points hydraulic actuator's. The loading method was selected the single side tension pad type to remove the upper loading side fixture. This single side loading method can be acquire the clear surface image to measure the skin deformation without obstruction of loading fixtures. Therefore, buckling deformations and strain distributions of the upper cover of PCWS can be measured by Digital Image Correlation (DIC) method. Many Strain gages and optical fibre sensors are installed to the PCWS which can be compare the design strain level between analysis and test. The PCWS is shown in Figure 27.

<Full scale test of PCWS>

Three major loading cases are prepared to conduct the static test for PCWS to evaluate the strength characteristics. The first loading case is strain survey of PCWS to check the loading and measuring systems at 20 % Design Limit Load (DLL). The second loading case is DLL test to evaluate the characteristics of the detrimental permanent deformation. Final case is Design Ultimate Load (DUL). Structural test program of PCWS is configured strain survey, impact test, static test fatigue test, non-destructive inspection, and repair. Structural Health Monitoring (SHM) by optical fiber sensor will applied to PCWS test program. This test program is scheduled to reach the final design ultimate load test in 2 years. The Damage Tolerance Test (DTT) is also scheduled at latter phase of the static test. The DTT is consisted from impact test, saw-cut test, and repair test. Fatigue test is also scheduled to measure the characteristics of the flight load cycle after the static test program. Test set-up image is shown in figure 28.

<Conclusion>

A 5m long Partial Composite Wing Structure (PCWS) was designed to demonstrate the full scale fabrication, assembly and structural test. VaRTM stitch composite was applied to the wing spar to eliminate the in-flight impact problem, complex shape drape

problem, and also cost. Electrical Heating Press Forming (EHPF) method was applied to titanium fitting of spar splice. Structural test program of PCWS is configured strain survey, impact test, static test fatigue test, non-destructive inspection, and repair. Structural Health Monitoring (SHM) by optical fiber sensor will applied to PCWS test program. This program aims to demonstrate the new technologies and to extract the technical problems of practical use. Now, final assembly and test set up of the Partial Composite Wing Structure is underway.

4. STRUCTURAL HEALTH MONITORING

4.1 Application of Distributed Fiber Optic Strain Sensors for Local Indentation/Impact Damage Detection in Foam Core Composite Sandwich Structures

Juho Siivola, Shu Minakuchi, Nobuo Takeda

The University of Tokyo

Foam core composite sandwich structures have gained attention in wide range of applications, including aircraft primary structures due to their attractive properties; light weight, high strength and stiffness, improved bending properties, multifunctionality, and reduced cost due to ease of manufacturing and low part count. Transverse loadings can however cause notable damage in the structures due to the thin face sheets and weak core. Furthermore, even if the core is notably damaged, only barely visible residual dent can remain on the face sheet under low-velocity impact or indentation loading. This can have notable effect on the residual strength and integrity of the structure (Fig. 29). A way to accurately detect and assess these kinds of damages is thus needed to ensure safe usage of the structures. In this study, optical fiber sensors are applied to foam core sandwich structures to monitor the strain distribution during and after indentation and low-velocity impact events. The strain information is used to identify the damage and to estimate its location and size.

As the residual dent in foam core sandwich structures after indentation/low velocity impact can be very small and shallow, a monitoring system with high resolution is needed to be able to detect the damages. For this purpose a Rayleigh scattering based

monitoring system is now used as it can provide distributed strain data with high spatial resolution. The optical fiber sensor was embedded between the face sheet and adhesive layer of the sandwich setup. This embedment location allows detection of strains caused by local bending of the face sheet and also possible strains from plastic deformation in the adhesive layer or in the core near the face sheet.

Monitoring ability of the system was studied experimentally by conducting indentation and low-velocity impact tests with sandwich specimens consisting of foam core and carbon fiber reinforced plastic face sheet joined together using an adhesive film. The strain distribution at the core-face sheet interface of beam and panel structures was monitored continuously during the indentation tests and before and after impact events by the optical fiber embedded in the adhesive layer. The system was also tested by low-velocity impact tests on a large scale sandwich panel simulating realistic applications. In addition, finite element analysis was conducted to verify the strain measurements and to compare the measured strain data with the predicted damage in the structure. Correlation between the predicted damage and measured strains thus provide a method to estimate the size of the barely visible damage from the strain data.

Based on the experimental data, it was shown that the monitoring system provided accurate and high resolution strain data during the loading events and after unloading (Fig. 30). From this strain data it was possible to detect indentation or impact induced damages from the residual strains remaining in the structure. Based on the finite element analysis observations, the damage core area could also be estimated from the strain data. Finally the performance of system was verified by monitoring low-velocity impacts on large scale sandwich panel, and it was confirmed that the used system can accurately measure the strain distribution in the foam core sandwich structures and detect even the smallest changes in residual strains that can be used to estimate the location and size of even barely visible damages.

This study therefore showed that the embedded optical fiber based monitoring system performs well and succeeded in damage detection of foam core sandwich structures. Furthermore, the high resolution strain distribution data used in this study indicates that the usage of the system is not only limited to damage detection, as it can also be useful for other measurement and monitoring purposes during design, manufacturing and service of the structures.

4.2 Development of Optical Fiber Sensor Based Impact Damage Detection System for Composite Airframe Structures

Noriyoshi Hirano¹, Hiroshi Mamizu¹, Akira Kuraishi^{1*},
Toshizo Wakayama¹, Nobuo Takeda², Kiyoshi Enomoto³

¹ *Kawasaki Heavy Industries, Ltd.*,

² *The University of Tokyo*,

³ *SOKEIZAI Center*

Airframe structures, especially composite structures, are prone to damage by tool drops, bird strikes, hailstones, etc. Structural health monitoring is helpful technique to maintain airworthiness from such impact damage by informing impact event and location, as well as impact damage level in in-flight condition. The authors have developed an optical fiber based impact damage detection system for composite airframe structure since 1998 in collaboration with the University of Tokyo and RIMCOF (SOKEIZAI Center at present) [1]. The system detects impact damage with two types of measurement methods, namely, (a) optical intensity measurement before and after impact events by multi-mode fibers and (b) strain measurement with multiple Fiber Bragg Grating (FBG) sensors (Fig.31). In method (a), impact damage can be detected with the optical intensity change associated with the extent of the impact damage such as matrix crack, delamination, or local deformation in the vicinity of the dent. In method (b), impact locations are detected from the arrival time difference of strains obtained with the multiple FBG sensors. Impact damage level can also be detected with the power spectrum density of the strain responses.

KHI has conducted more practical studies toward real aircraft application with taking into account the economical and business issues [2]. KHI assessed the impact detectability through series of impact tests using several types of specimens ranging from coupon to component levels following the building block approach. In addition, environmental durability was evaluated to assess the Technology Readiness Level (TRL) of the system. The environmental durability tests covered wide range of conditions assumed to be exposed in aircraft operation such as temperature, humidity, hydraulic fluid, fuel and so on. As an installation study, sensor installation patterns were studied for a representative single aisle jetliner using 3D CAD (Fig.32). As a

manufacturing and maintenance enhancement, the repair method of embedded optical fiber was developed.

Although the localization errors mentioned above result were within acceptable level, there is still room for improvement [3]. To assess the optimal FBG sensor direction for higher localization accuracy, KHI performed impact tests using CFRP stiffened panel imitated an actual aircraft structure (Fig.33). The panel includes 12 FBG sensors aligned in three directions (in effect, similar to a rosette type strain gage). The novel FBG sensor monitoring system of 800 kHz sampling developed by Anritsu corporation was used in the impact tests. The result shows the frame direction sensor is more sensitive and suited for localization. The improvement of impact damage level detection is necessary as well if the system is to supplement the conventional non-destructive inspection such as ultrasonic inspection that is widely used in aircraft industries, but labor intensive and costly. To assess useful signals for estimating impact energy or impact damage level, high frequency domain of power spectrum density (PSD) obtained by 800 kHz sampling was studied in detail [3]. It is found that the PSD integral over 1 kHz is more suited for estimation of dent depth and/or damage area, more so than the impact energy.

This work was conducted as a part of the project, "Advanced Materials & Process Development for Next-Generation Aircraft Structures" under the contract with SOKEIZAI Center, founded by Ministry of Economy, Trade and Industry (METI) of Japan.

References

- [1] H.Tsutsui, A.Kawamata, J.Kimoto, A.Isoe, Y.Hirose, T.Sanda, N.Takeda, "Impact damage detection system using small-diameter optical-fiber sensors embedded in CFRP laminate structures", *Adv. Composite Mater.*, 13(1), 43-55 (2004).
- [2] N.Hirano, R.Yoshimura, J.Kimoto, T.Itoh, N.Takeda, M.Yoshida, "Development Status of Optical Fiber Sensor based Impact Damage Detection System for Composite Airframe Structures", *Proceedings of 9th International Workshop on Structural Health Monitoring-2013*, (DVD)

[3] N.Hirano, H.Mamizu, A.Kuraishi, T.Itoh, N.Takeda, K.Enomoto, “Detectability Assessment of Optical Fiber Sensor based Impact Damage Detection for Composite Airframe Structure” Proceedings of European Workshop on Structural Health Monitoring-2014, (DVD)

4.3 Development of Ultrasonic Based Structural Health Monitoring (SHM) Technology with MFC and FBG Hybrid Sensor System for Aircraft Structures

Kouhei Takahashi¹, Hideki Sejima¹, Megumi Hiraki¹, Yoji Okabe², Nobuo Takeda², Hiroto Kojima³

1, Fuji Heavy Industries Ltd., 2, The University of Tokyo, 3, SOKEIZAI Center

We have been developing a Structural Health Monitoring (SHM) system for aircraft structure to reduce maintenance cost and to improve safety and weight performance. Although Carbon Fiber Reinforced Plastic (CFRP) material has many advantages against conventional metal materials, debonding and delamination in CFRP structures would not be detected easily and this drawback makes adverse effect against reducing structural weight. Our SHM system can analyze structural integrity by evaluating changes in the shape of the measured Lamb wave[1]. The Lamb wave, a type of ultrasonic wave, is oscillated by a Micro Fiber Composite (MFC) piezoelectric actuator, then the wave propagates in the structure and is detected by a Fiber Bragg Grating (FBG) optical fiber sensor as shown in figure 34. Maintenance cost will be reduced by the SHM system since inspection procedure would be conducted by ground support equipment and it doesn't required direct access for the structures.

In our latest work, the SHM system was installed into repaired region to diagnose bonding integrity and to detect occurrence and shape of debonding. Patch repair is one of the most common repair procedures for CFRP structures and there will be many concerns about increase of maintenance cost for periodic inspection with increasing number of repair process. Therefore, installing the SHM system into the repaired region makes inspection procedures high efficiency. Figure 35 shows schematic of the specimen, sensor configuration and results of the test. The specimen was simulated skin/stringer stiffened panels of aircraft structures and a repair patch was bonded on the outside of panel. Debonding between skin and repaired patch was introduced and propagated artificially, then the SHM system diagnosed the debonding condition. As a

results of the test, we confirmed that the SHM system could detect occurrence of debonding and propagation of debonding approximately. This results show that only conventional NDT is required when the SHM system detect any damages and introduction of the SHM system would make the inspection procedure more flexible and less expensive. Moreover, the SHM system will be developed as a technology which can monitor the structural integrity during flight condition in the future.

Reference

[1] K. Takahashi, et al, “Damage detection technology for CFRP structure using MFC/FBG hybrid sensor system”, Proc. 9th International Workshop on Structural Health Monitoring 2013 , pp. 2027-2034, 2013.

5. LIFE EVALUATION ANALYSIS

5.1 Bayesian Approach to Load Enhancement Factor

Seiichi Ito¹, Sunao Sugimoto², Yuichiro Aoki² and Takao Okada²

¹*Japan Aerospace Technology Foundation*

²*Japan Aerospace Exploration Agency*

Load enhancement factor(LEF)

The load enhancement factor (LEF) approach is proposed as a fatigue acceleration test to demonstrate the fatigue strength of composite material structures. The objective of the LEF approach is to increase the applied loads in the fatigue spectrum so that the same level of reliability can be achieved with short test durations. Some fatigue tests on the full-scale composite structure are executed on the basis of this method. In the LEF approach, the probability distribution of residual strength r and fatigue life L is assumed to be a two-parameter Weibull distribution, $W(r|\alpha_r, \beta_r)$ and $W(L|\alpha_L, \beta_L)$, respectively. LEF is defined as a function of shape parameters from the Weibull distributions. A final mathematical relationships of LEF is shown by equation (1).

$$LEF(\alpha_r, \alpha_L) = (N_F / N_T)^{\alpha_L / \alpha_r} \quad (1)$$

where N_F is the mean value of fatigue life and N_T indicates the fatigue test duration. As a consequence, the uncertainty in residual strength and fatigue life greatly affects LEF assessment. For simplicity, modal values of the shape parameters are used in the Composite Materials Handbook (CMH-17).

Expected value of LEF

This study investigates the uncertainty in the shape parameters in more detail. First, the shape parameters are modeled as a probability distribution, by using Bayesian analysis to evaluate the scatter of the shape parameter. As the so-called parametric method, the unknown parameters of the distribution are estimated using the Bayesian method from the database. The Bayesian expected value of LEF is calculated from the estimated posterior probability distributions of the shape parameter, $f_{\alpha_r}(\alpha_r)$ and $f_{\alpha_L}(\alpha_L)$:

$$\underline{LEF} = \iint_{\alpha_r, \alpha_L} LEF(\alpha_r, \alpha_L) f_{\alpha_r}(\alpha_r) f_{\alpha_L}(\alpha_L) d\alpha_r d\alpha_L \quad (2)$$

When the uncertainty of the shape parameter is large and the assumption of the usual probability distribution is problematic, the non-parametric estimation method for the distribution is applied. The probability distribution approximation that uses the spline function and Bayesian method is used here. In this case, the posterior distributions in equation (2) are replaced by the probability distribution function obtained the non-parametric method. This paper presents two types of expected LEF values mentioned above and their comparison with already reported results in CMH-17. These comparison results are shown in Table 2.

LEF based on lognormal distribution

Since the scatter of the fatigue life is large, the lognormal distribution is also a basic probability model. Then, LEF that assumes lognormal distribution for residual strength r and fatigue life L is formulated as follows:

$$LEF(\sigma_r, \sigma_L) = (N_F / N_T)^{\sigma_r / \sigma_L} \quad (3)$$

where σ_r and σ_L are the standard deviation of lognormal distribution for r and L , respectively. The standard deviation s of the common logarithm to the Weibull variable is in inverse proportion to the Weibull shape parameter:

$$\alpha = \pi / (\sqrt{6} \ln 10 \cdot s) \quad (4)$$

Then, equation (3) is also analogized from this relation.

6. FULL SCALE TESTING

6.1 XP-1&XC-2 Strength Test/ ATD Strength Test/ Crashworthiness Technology

T. Okazaki

*Air Systems Research Center, Technical Research and Development Institute (TRDI),
Ministry of Defense*

1. XP-1&XC-2 Strength Test

Since 2001, TRDI has been conducting a simultaneous development of the next-generation maritime patrol aircraft (XP-1) which is the successor to P-3C operated by Japan Maritime Self-Defense Force and the next-generation cargo aircraft (XC-2) which is the successor to C-1 etc. operated by Japan Air Self-Defense Force.

The development of XP-1 has successfully completed in March, 2013. The structural integrity of XP-1 was finally verified by three full scale strength tests (Refer to Fig.36 (left)) which were the static test (included 12 load conditions for rigidity, 71 load conditions for limit load, and 72 load conditions for ultimate load), the durability test under spectrum loading equivalent to two design service lifetimes, and the damage tolerance test under spectrum loading equivalent to two design service lifetimes with initial cracks at 38 locations followed by the residual strength test (three load conditions). Two full scale test articles delivered in 2006 and 2007, one is for the static test and the other is for the durability test and the damage tolerance test, were used for these strength tests.

In the development of XC-2 the strength test has been continued to verify the strength of XC-2 airframe (Refer to Fig.36 (right)).

2. ATD Strength Test

Advanced Technology Demonstrator (ATD) is an experimental aircraft designed for evaluating the maturity and integration of advanced airframe and engine technologies for future fighters.

This project was started in 2009, and the full scale static strength test was also started by TRDI (Refer to Fig.37).

3. Crashworthiness Technology

In order to improve the survivability of occupants during a vertical crash of a helicopter, the helicopter cabin-component which had composite absorbers in the subfloor and protective frames for crew was designed and fabricated (Refer to Fig.38). The cabin-component with a dummy occupant was dropped at a vertical impact speed that MIL-STD-1290A required for helicopter crashworthiness. Consequently, it was shown that the cabin-component successfully decreased acceleration and maintained a survivable volume for occupants during the crash impact. Thus, the crashworthiness structure for a helicopter was successfully demonstrated.

6.2 Curved Panel Fatigue Test for MRJ-200 Pressurized Cabin Structure

Kaoru Tsukigase¹, Toshiyasu Fukuoka¹, Keisuke Kumagai¹, Toshio Nakamura²,
Shunsuke Taba²

¹*Mitsubishi Aircraft Corporation*

²*Mitsubishi Heavy Industries, LTD.*

Widespread fatigue damage is a well-known complex fatigue phenomenon. To prevent widespread fatigue damage, FAA has issued 25.571 amendment 25-132 and Part 26 subpart C in late 2010, and they became effective in January 2011. To comply with the new regulatory requirement, full-scale airplane fatigue test of MRJ-200 will be conducted by simulating actual airplane structural configuration with a typical operation loads expected in service to show free from widespread fatigue damage in operational life. In order to find out the fatigue characteristics of the fatigue critical structure in early stage of MRJ-200, the sub-component level fatigue tests to evaluate widespread fatigue damage are planned. In the susceptible structures, fuselage cabin pressurization area focused in early substantiation activity. For damage tolerance evaluation for MRJ-200, a lot of coupon/element/component tests are conducted to support analysis. Since full-scale airplane fatigue test will be utilized for widespread fatigue damage evaluation, the crack growth evaluation of fuselage structure with bulge effect and stiffness effect will be conducted by sub-component test simulating cabin pressure in conjunction with axial loading due to fuselage bending.

For the widespread fatigue damage and damage tolerance evaluation for MRJ-200, the test fixture for sub-component level tests has been developed to demonstrate fatigue cyclic loading under cabin pressure and axial load (Figure 39). As main focus of this test fixture concept, negative pressure loading is used to simulate differential pressure load between inside cabin and outside. This fuselage curved panel fatigue test fixture using negative pressure takes some benefits (Figure 40). First one is test loading speed which can be accelerated by minimized pressure tight case. Second one is safety. In principle, the pressure higher than atmosphere pressure can't be applied on test panel, therefore test panel has less risk for dangerous bursting. Using this test fixture, several curved panel fatigue tests for fuselage critical area to fatigue are planned as early substantiation activity for widespread fatigue damage and damage tolerance evaluation.

7. MISCELLANEOUS

7.1 An Amphibian and the Concept of Its Derivative Model for Firefighting

Application

Masatoshi Tsujii, Hideyuki Mochida, Katsuo Tanaka,
Atsuhiko Fujitani, Yushi Goda,
ShinMaywa Industries, Ltd.

The history of seaplanes

In 1910, 7 years later than the first flight of the Wright brothers, the world's first flight of seaplane was achieved by Henri Fabre in France. Since then, seaplanes have achieved technical advances through various opportunities including the famous seaplane race "the Schneider Trophy." Consequently in 1930s, large seaplanes were adopted for long distance flight. After the establishment of landing gear technology and the development of airports worldwide, their role as passenger transports was taken over by landplanes, however, seaplanes still play important roles in various applications, such as aerial firefighting, search and rescue on the sea.

The postwar history of amphibian development by ShinMaywa

Following the lifting of the ban on aircraft development and manufacturing in Japan, which had been imposed during the US occupation after the Second World War, ShinMaywa proceeded with the development of a new amphibian. With the UF-XS experimental plane, which was modified from the Grumman UF-1 provided by the US Navy, ShinMaywa pursued the studies of new technologies such as the hull design of high seaworthiness and the Boundary Layer Control (BLC) system, which were adopted in the PS-1 Anti-submarine Flying Boat. The PS-1 then developed into its derivative model the US-1/US-1A Search and Rescue Amphibian, and made further progress to the latest US-2 Search and Rescue Amphibian.

The features of the US-2 Search and Rescue Amphibian (Fig.41)

With keeping the advantages of its predecessor US-1A, such as high seaworthiness and the capability to cruise at extremely low speeds, the US-2 has various improved features, including the pressurized cabin, fly-by-wire control system, the glass cockpit and the enhancement in power by the conversion of engines and propellers, which led to the improvement in comfort for patients, the operability and the performance. The US-2 is the world's only search and rescue amphibian that can land on water with waves up to three meters high.

The concept of firefighting application (Fig.42)

Against the backdrop of the fact that seaplanes are being used for aerial firefighting operation in some foreign nations, the study to convert the US-2 for this application is ongoing. To enable releasing water in the air to extinguish fires, the fuel tank in the fuselage is planned to be converted into the water tank with the additional door provided at the bottom of hull to drop the water. The US-2 Firefighting Amphibian would be the unrivaled firefighting aircraft that can carry about 15 tons of water and deliver it while cruising at extremely low speeds.

The concept of structural integrity evaluation

Corrosion due to seawater can be cited as a cause for damage specific to amphibious aircraft. ShinMaywa has unique techniques for corrosion protection with long experience as an amphibian maker. One of the techniques is unique coating system for

corrosion prevention. It is applied to parts that are prone to corrosion, such as bilge structure. In addition, ShinMaywa's amphibians have On-board Engine Washing System to prevent the main engines, APU (Auxiliary Power Unit), and BLC from salt accumulation and corrosion. This system realises on-board washing of the engines on the sea or in-flight during operations. Also, the entire aircraft is washed after operations if water landings are performed.

In spite of the above, it is still very difficult to prevent corrosion perfectly. So, it is important to consider the structural integrity for corrosion damage. When some corrosion is detected and removed, structural member is reinforced because removal of corrosion leads to decrease in thickness of structural member. ShinMaywa considers that it is possible to develop an original analysis model that is suitable for amphibian by reflecting the influence of thickness decrease and reinforcement to Fatigue and Damage Tolerance analysis model. Currently, it is planned to monitor the corrosion status and thickness decrease regarding in-service US-2. ShinMaywa intends to select structural critical points that should be monitored in preparation for the analysis model development.

7.2 Development of Test and Analysis Methods for Lightning Strike on CFRP Structures

- Current Density Analysis : Takayuki NISHI, Hiroyuki TSUBATA (Fuji Heavy Industries LTD.)
- Spark Detection Technology : Shinya Ohtsuka (Kyushu Institute of Technology)
- Electric Charge Analysis : Kunihiko HIDAKA, Akiko KUMADA (The University of Tokyo)
- Multi-Layer Current Density Analysis : Yoshihiro BABA (Doshisha University)

The lightning protection technology has been developed as an important issue of aircraft design. Especially, due to the expansion of CFRP application to airframes, new lightning protection designs are required. In order to develop more affordable and rational designs, lightning current density analysis which can simulate fiber dominate phenomena for CFRP material and more efficient ignitable spark detection technology as tools for the designs have been developed. Also the analysis method of electrostatic charges as another sparking source in CFRP fuel tank structure is developed.

It is difficult to predict accurate current distribution considering fiber dominant properties using conventional current density analysis method. Therefore, the new analysis method with triangular prism cells in Finite Difference Time Domain (FDTD) simulation was developed, which can define not only 0deg./90deg. but also +45deg/-45deg for each layer shown in the right side of Fig.43. On the other hand, the experimental data also shows the fiber dominant current distribution by thermal images in the left side of Fig.43.

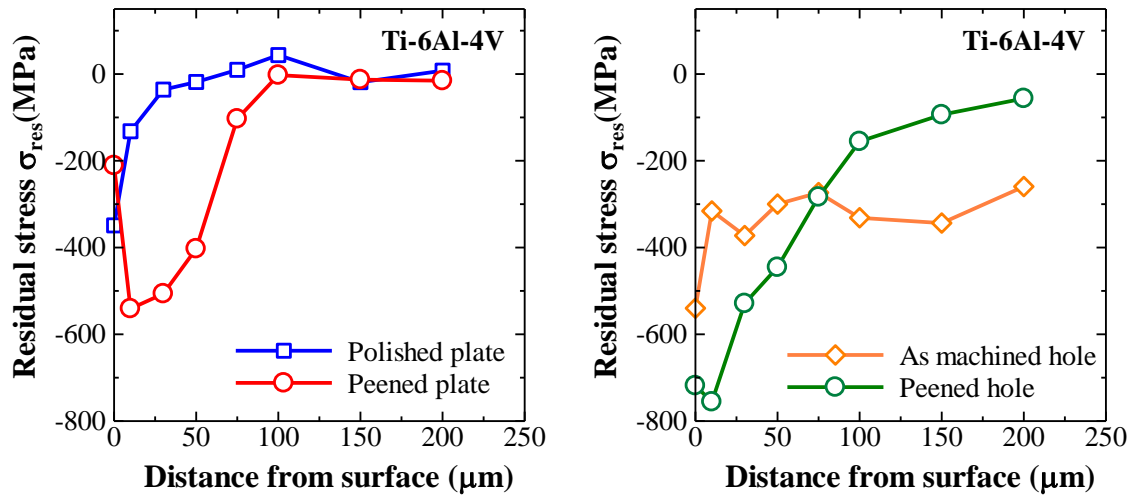
The ignitable spark detection technology using optical fiber and photo-multiplier tube has been developed. Figure 44 shows an example of measured image of the ignitable spark and estimated spark energy by the developed spark detection technology. The new method and system has higher accuracy and efficient process than conventional method by visual judgment using digital camera.

Applying the new current density analysis method for the lightning protection design and the efficient ignitable spark detection technology will make the design of the composite structures more accurate and efficient in the future.

ACKNOWLEDGEMENTS

The editors appreciated the members of the ICAF national committee of Japan Society for Aeronautical and Space Sciences, for their contribution in preparation of this national review and continuing discussion in the committee.

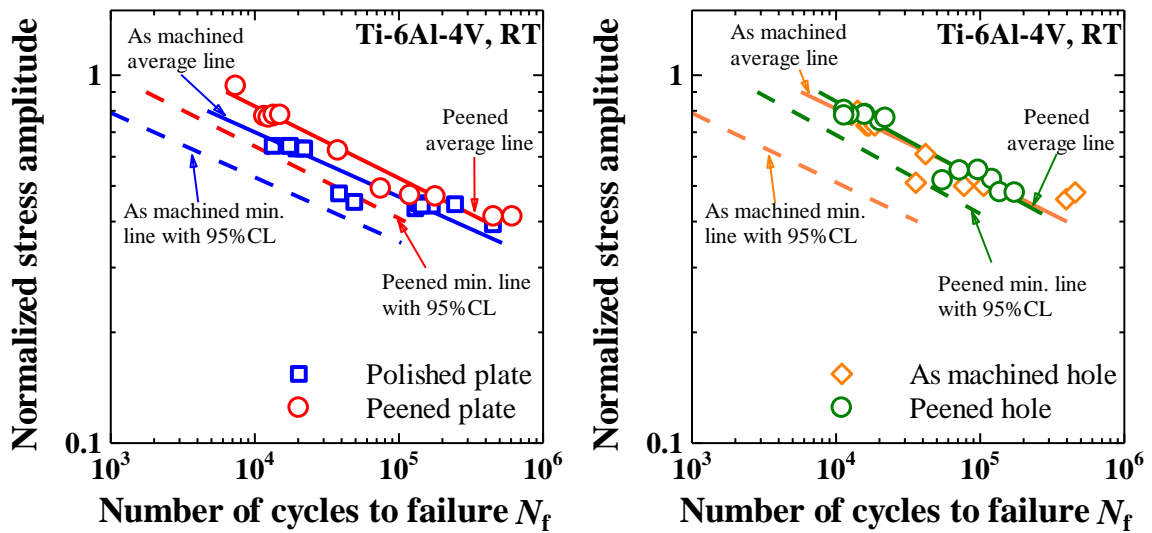
TABLES AND FIGURES



(a) Polished and peened plate.

(b) As machined and peened hole.

Fig.1 Residual stress distribution of as machined and peened specimen.



(a) Polished and peened plate.

(b) As machined and peened hole.

Fig.2 LCF test results of as machined and peened specimen.

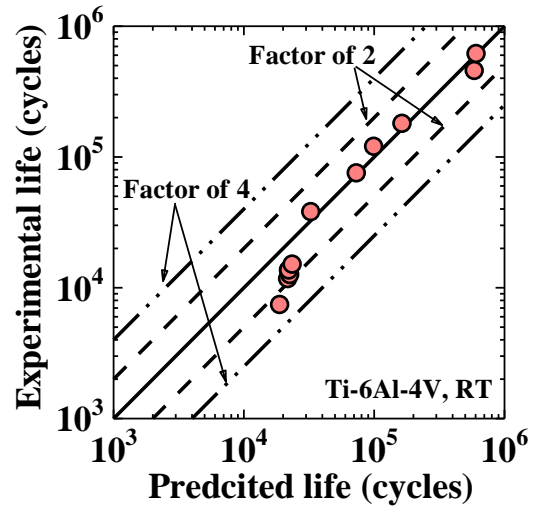


Fig.3 LCF life prediction based on crack growth analysis.

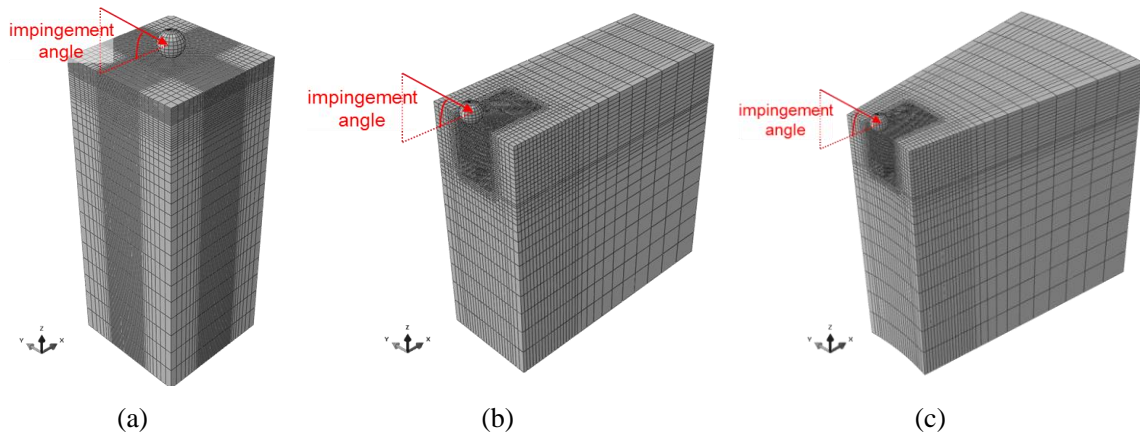


Fig.4 Single shot simulation finite element model for (a) flat surface, (b) edge feature and (c) hole feature.

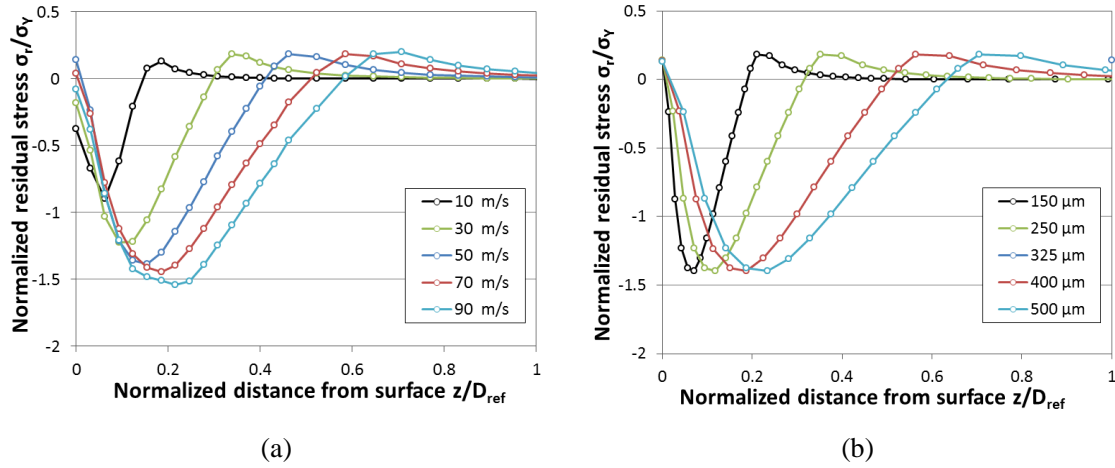


Fig.5 Example of residual stress distributions based on single shot simulation for (a) different impact velocities and (b) different shot sizes. Residual stress and distance from the surface are respectively normalized by the yield stress σ_Y and a reference shot diameter D_{ref} .

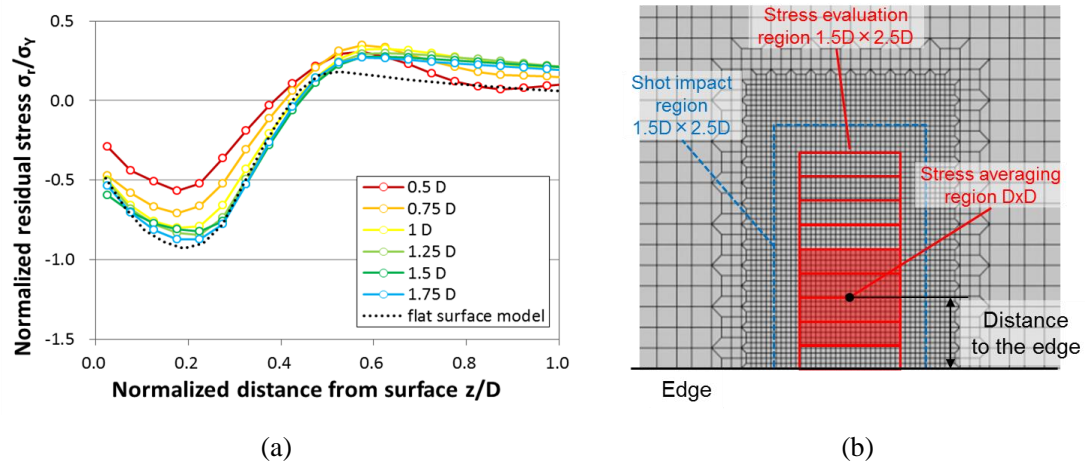


Fig.6 (a) Normalized residual stress profiles obtained from multiple shot simulation of the edge feature model and given for different distance to the edge. The residual stress are averaged over a region of area $D \times D$ as shown in (b), where D is the shot diameter. The distance to the edge (0.5 D to 1.75 D) refers to the distance between the edge and the center of the averaging area.

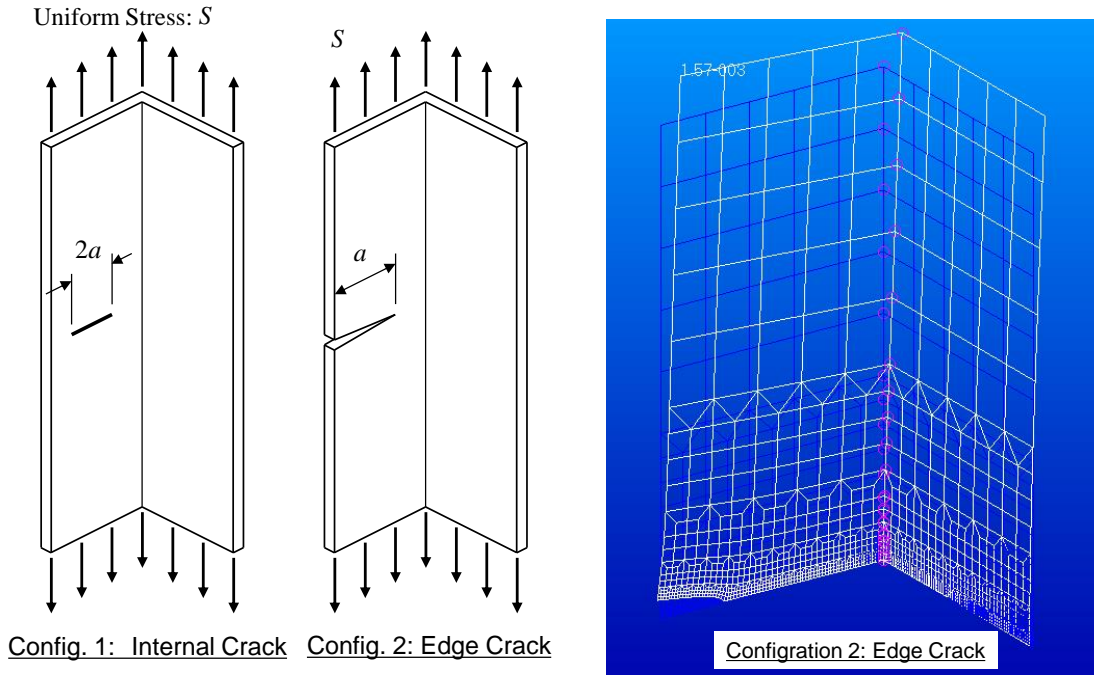


Fig. 7 Cracks in Angle Shaped Section and NASTRAN Model for Edge Crack

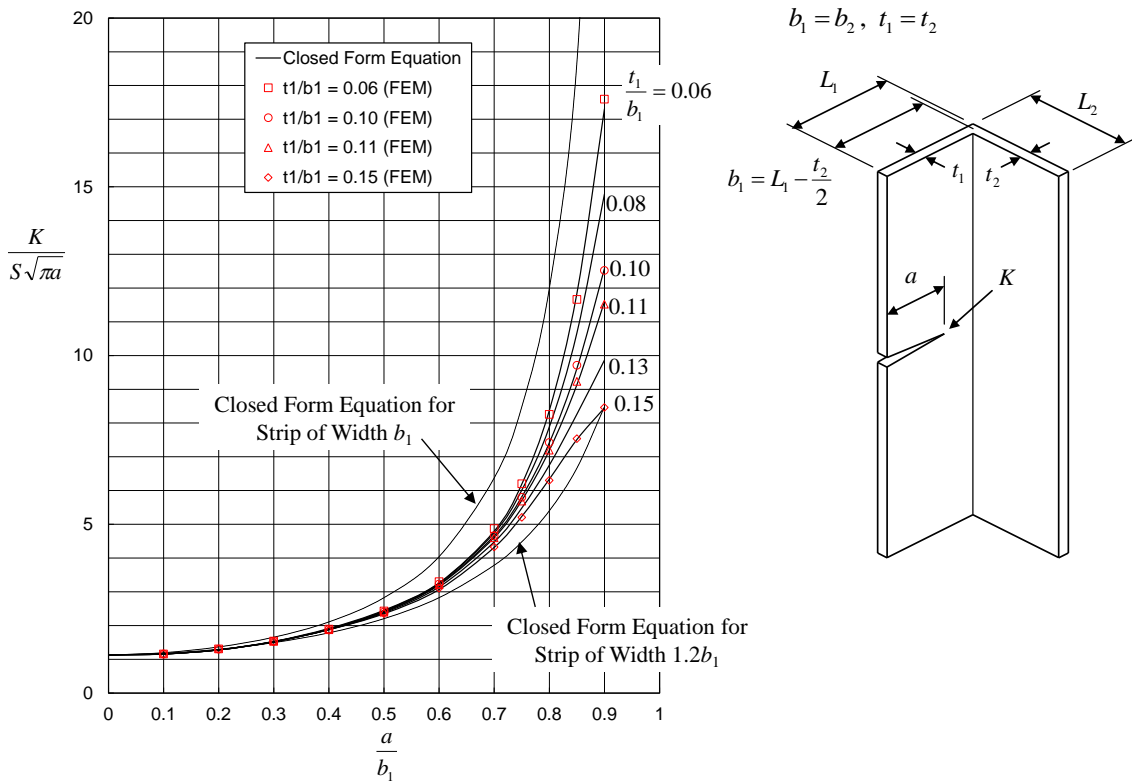


Fig. 8 Stress Intensity Factor for Edge Crack in Angle with Equal Width and Thickness

For Angle with Equal Width and Thickness: $b = b_1 = b_2, t = t_1 = t_2$

$$\beta = \frac{K}{S\sqrt{\pi a}} = c_0 + c_1\left(\frac{a}{b}\right)^{2.5} + c_2\left(\frac{a}{b}\right)^5 + c_3\left(\frac{a}{b}\right)^{7.5} + c_4\left(\frac{a}{b}\right)^{10}$$

$$c_i = a_{0i} + a_{1i}\left(\frac{t}{b}\right) + a_{2i}\left(\frac{t}{b}\right)^2, \quad i = 0, 1, 2, 3, 4$$

Applicable Range: $0.06 \leq t/b \leq 0.15$

c_i	a_{0i}	a_{1i}	a_{2i}
Coefficients for c_0	1.12739	0.168082	-1.12626
Coefficients for c_1	9.76981	-34.0904	195.587
Coefficients for c_2	-11.9628	135.332	-1361.02
Coefficients for c_3	-12.2707	402.640	800.461
Coefficients for c_4	88.2988	-1199.98	1974.17

Fig. 9 Closed Form Equation of SIF for Edge Crack in Angle with Equal Width and Thickness

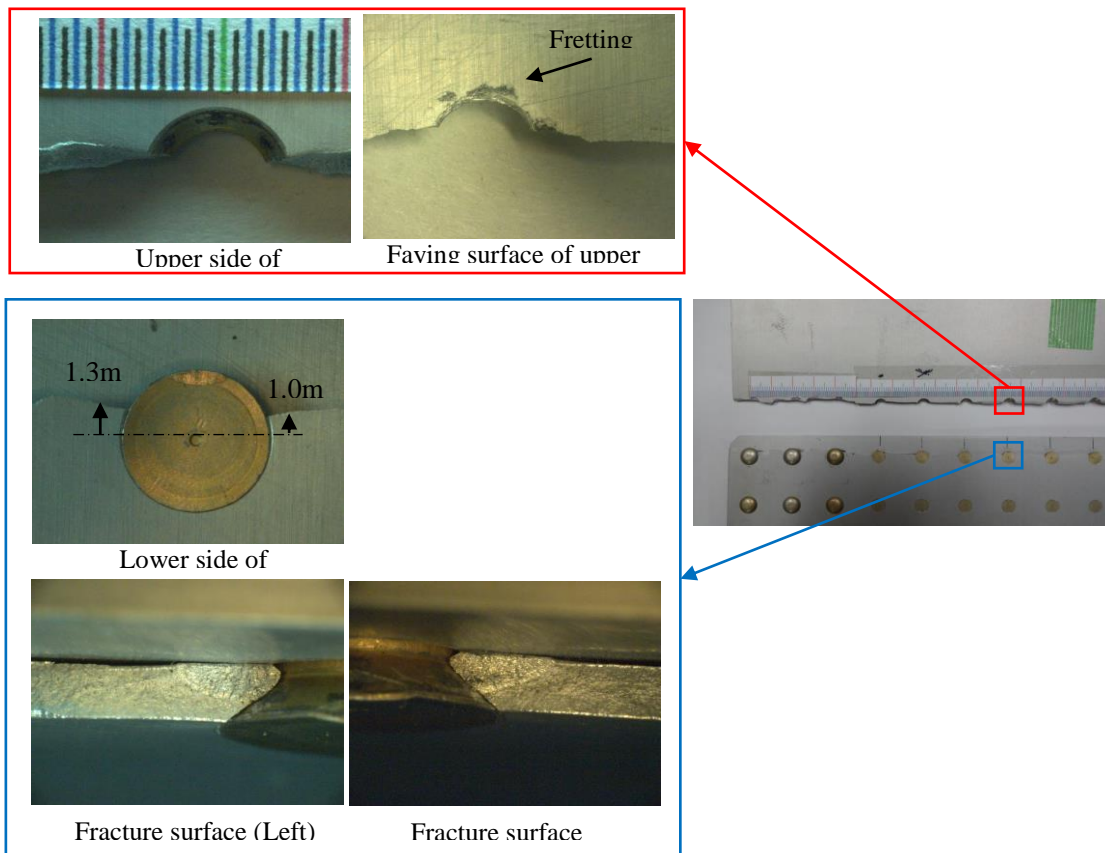


Fig. 10 Example of crack nucleation locations and fracture surfaces

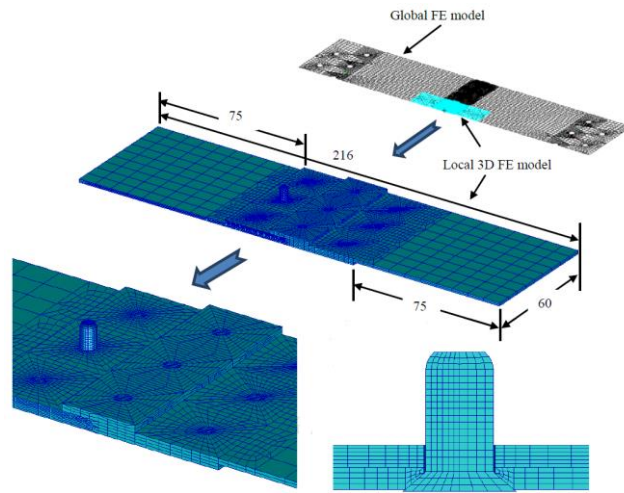


Fig. 11 FE model used in the numerical analysis

Skin: 2024-T3 CLAD (t=1.27mm)
 Rivet: NAS1097AD5, 5/32

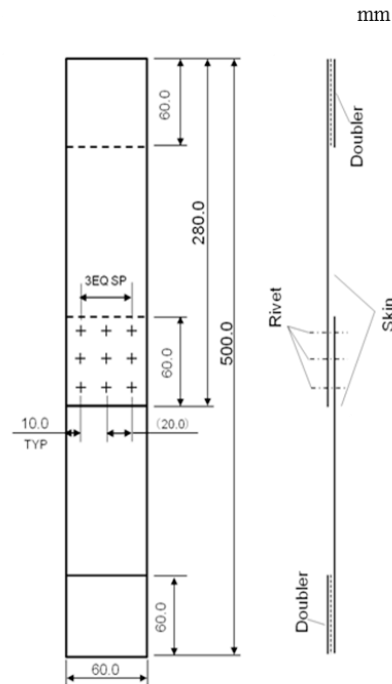


Fig. 12 Test Specimen

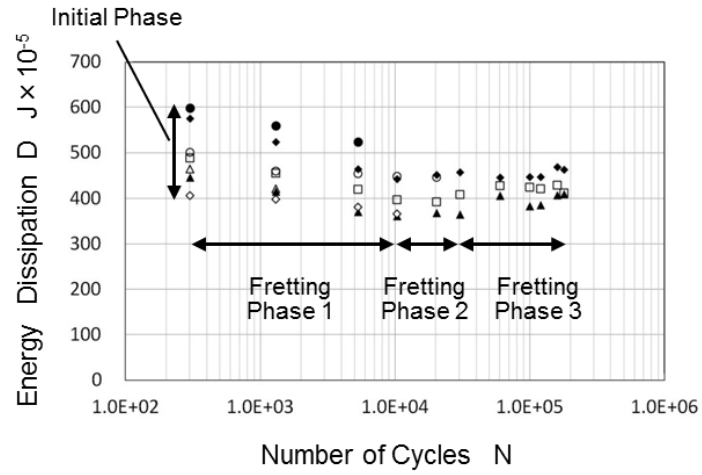


Fig. 13 Energy Dissipation vs. Number of Cycles of 7 Specimens

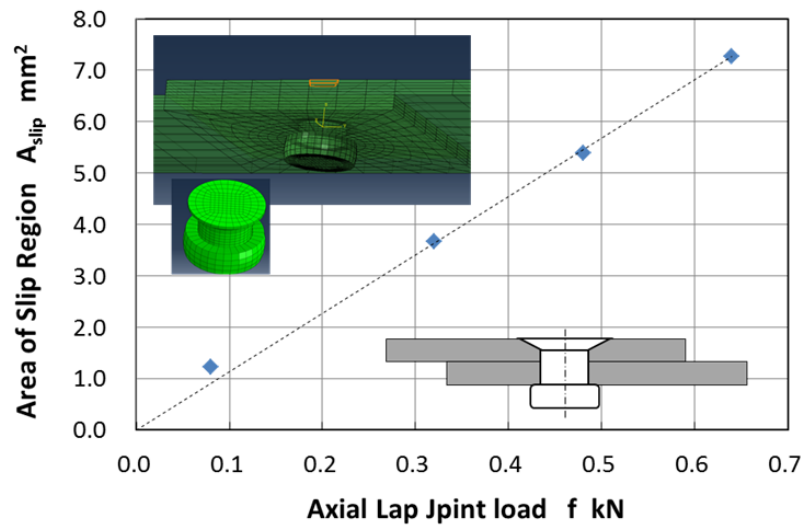


Fig. 14 Growth Rate of Slip Region by FEA.

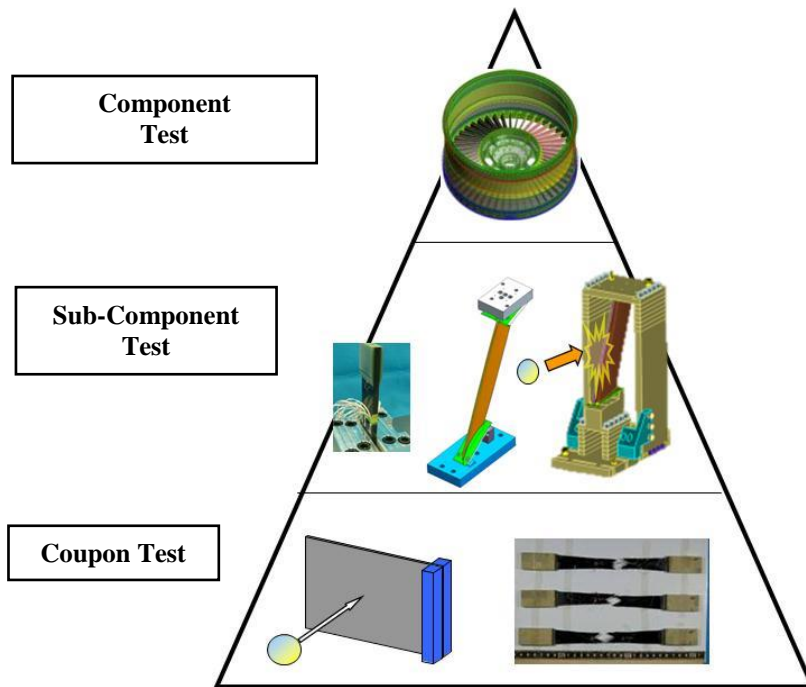


Fig. 15 Building block approach for composite SGV

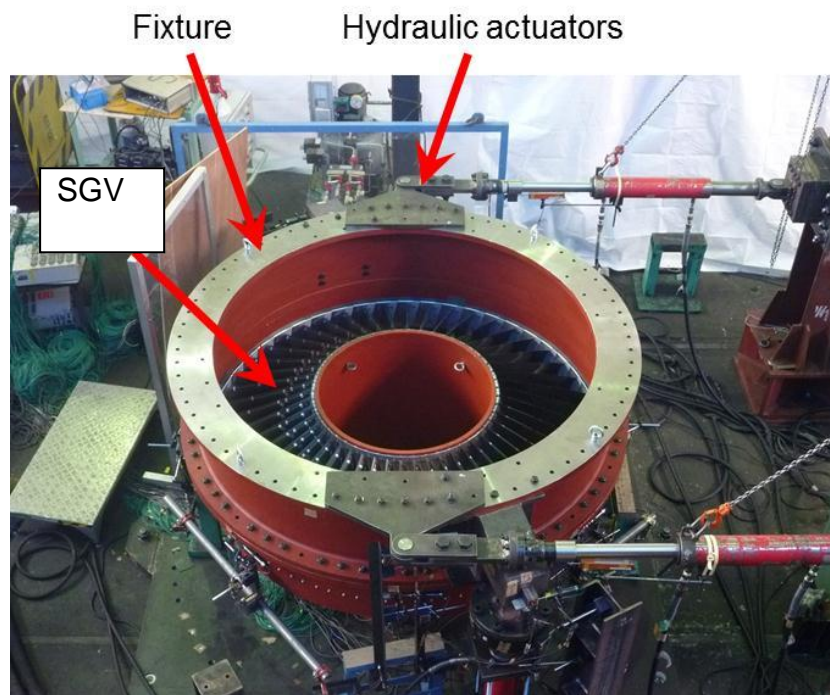


Fig. 16 Full ring test

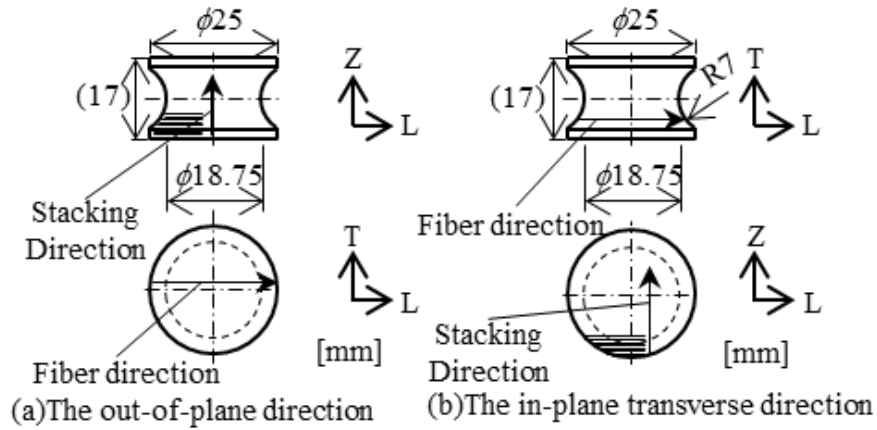


Fig. 17 Schematic illustration of pool specimens

Table 1 Mechanical properties of specimens

	Out-of-plane direction	In-plane transverse direction
Number of specimens	5	5
Failure stress σ_b MPa	45.7 (3.80)	59.5 (7.32)
Failure strain ε_b %	0.855 (0.0776)	1.07 (0.155)
Apparent elastic modulus E_{app} GPa	5.90 (0.107)	6.09 (0.0658)

* Values in parenthesis indicate the standard deviation

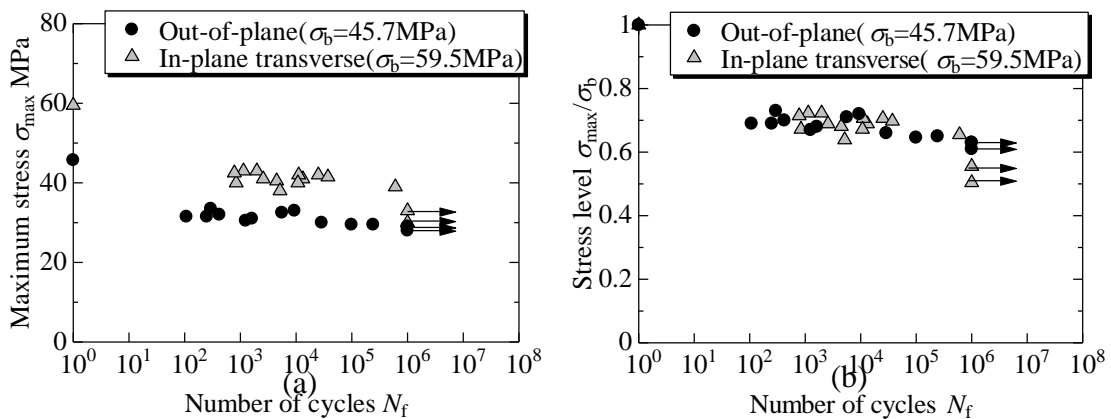


Fig. 18 S-N curve of the thick CFRP laminates with toughened interlaminar in the out-of-plane and the in-plane transverse directions: (a) with maximum stress; (b) with normalized stress.

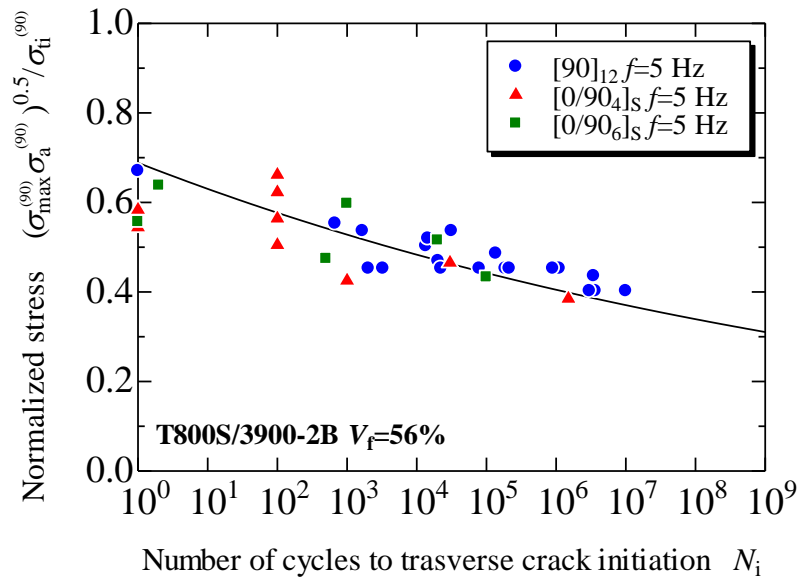


Fig. 19 Evaluation of the fatigue life to the transverse crack initiation of the laminates formed of T800S/3900-2B prepreg using a modified SWT model.

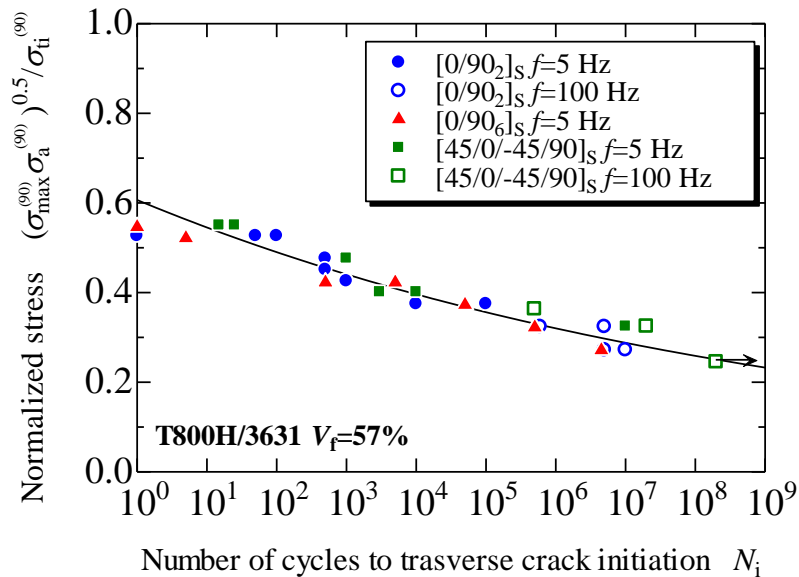


Fig. 20 Evaluation of the fatigue life to the transverse crack initiation of the laminates formed of T800H/3631 prepreg using a modified SWT model.

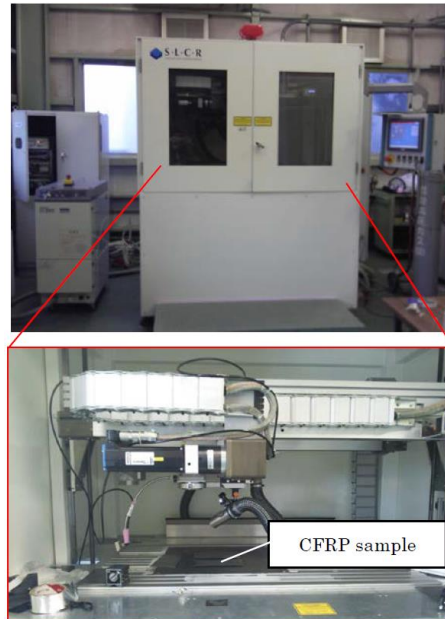


Fig. 21 Overview of pulsed laser processing

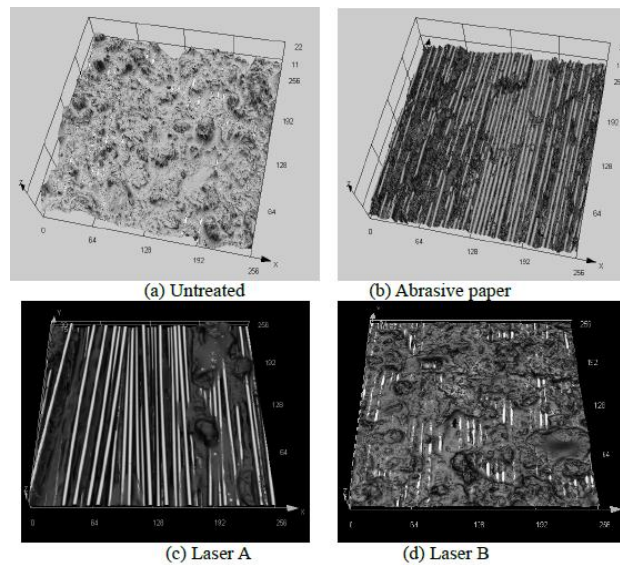
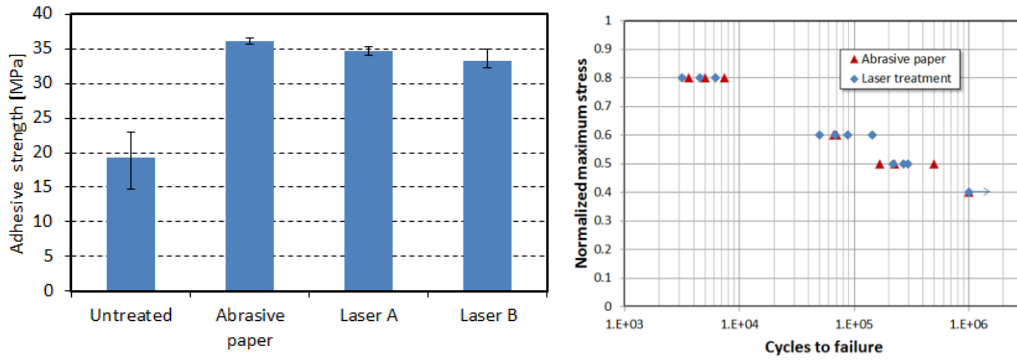
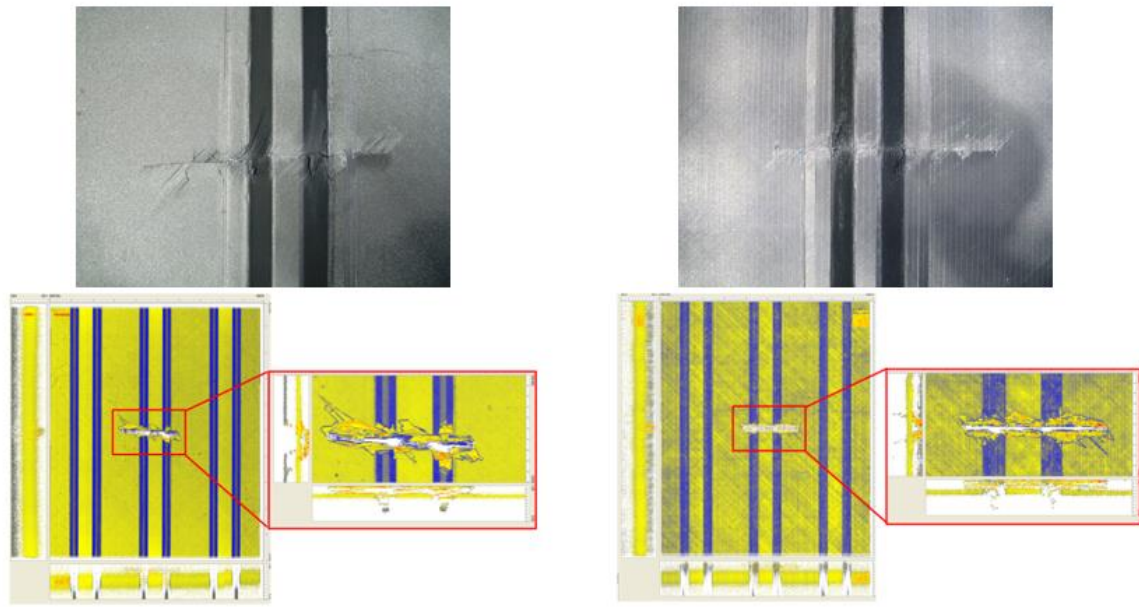


Fig. 22 Microscopic surface views of treated CFRP samples
(scale: $256\mu\text{m}\times 256\mu\text{m}$)



(a) lap-shear static strength (b) lap-shear fatigue strength

Fig. 23 Comparison of adhesive lap-shear strength



(a) Autoclave panel (b) VaRTM apnel

Fig. 24 Two-bay notch damage and NDT results

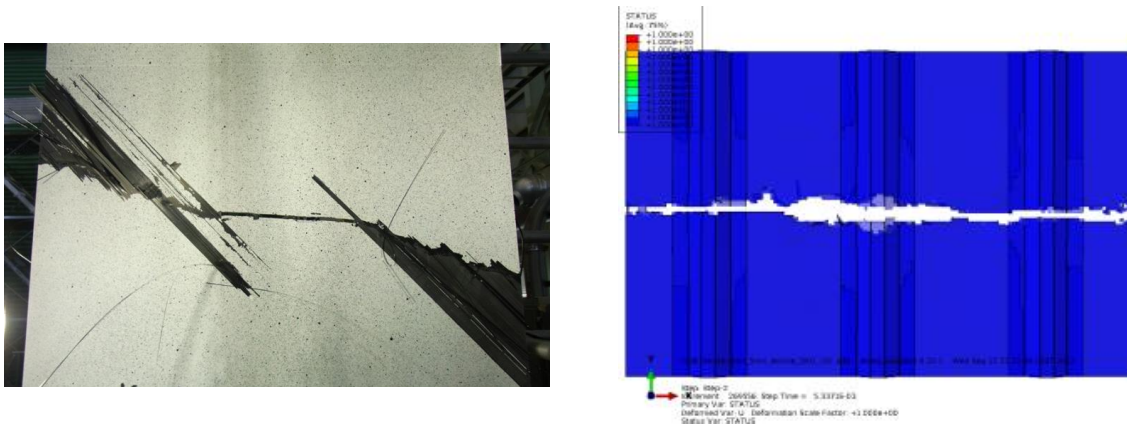


Fig. 25 Comparison of failure mode after residual tensile strength test

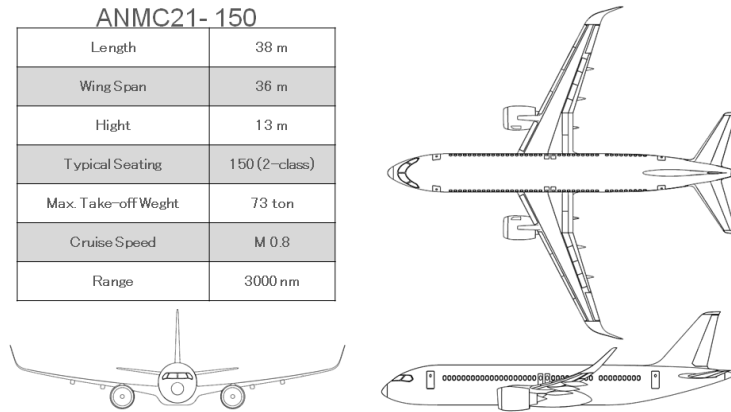


Fig. 26 Conceptual aircraft.

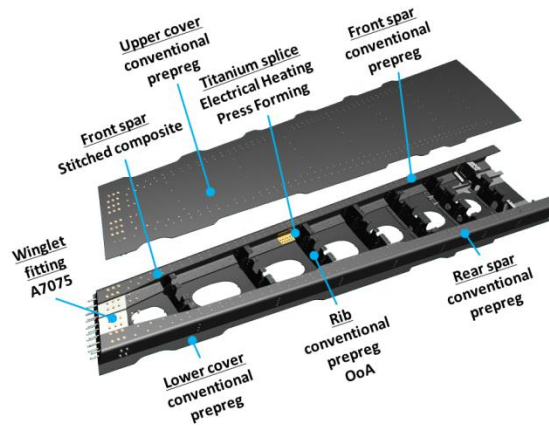


Fig. 27 Schematic of the partial composite wing structure.

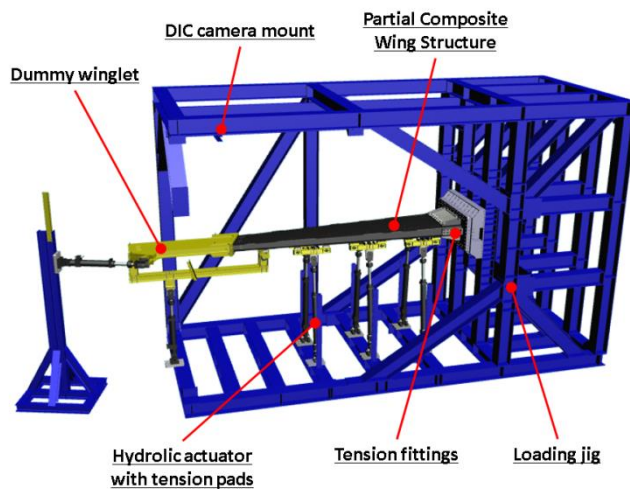


Fig. 28 Digital image of test set-up.

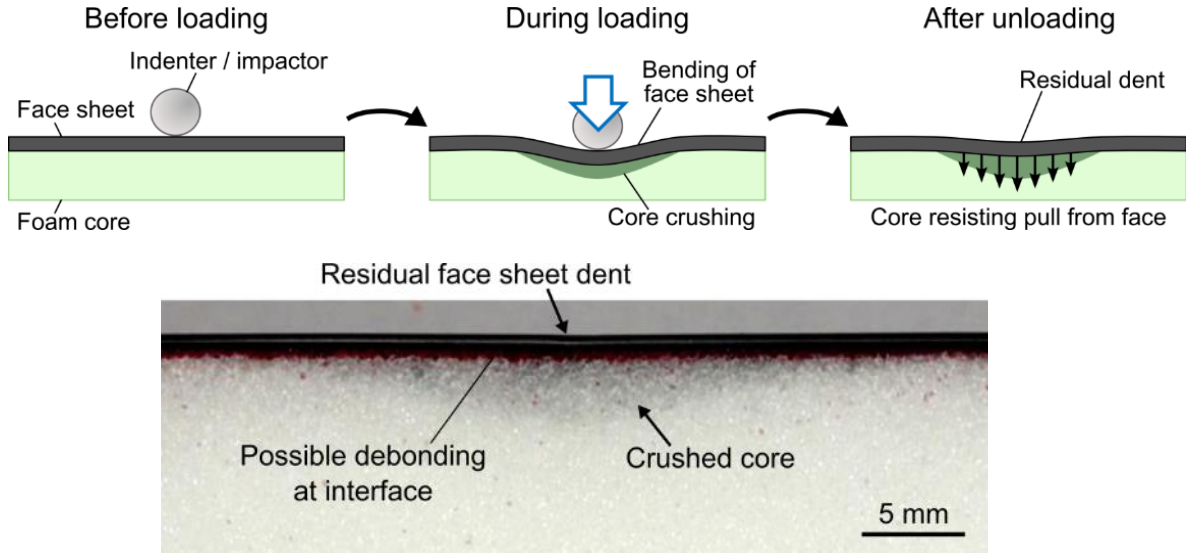


Fig. 29 Indentation damage in CFRP foam-core sandwich structures

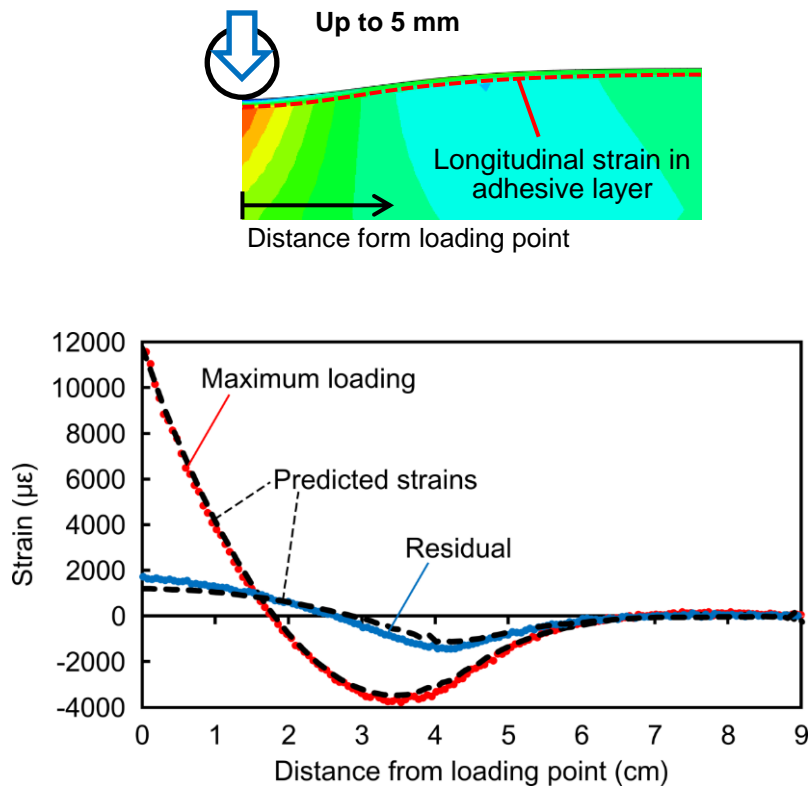
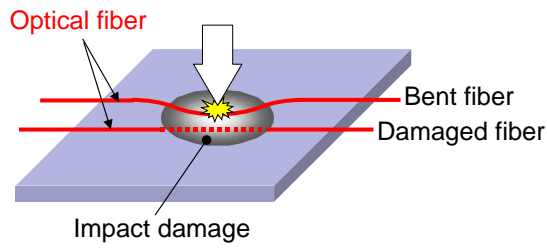
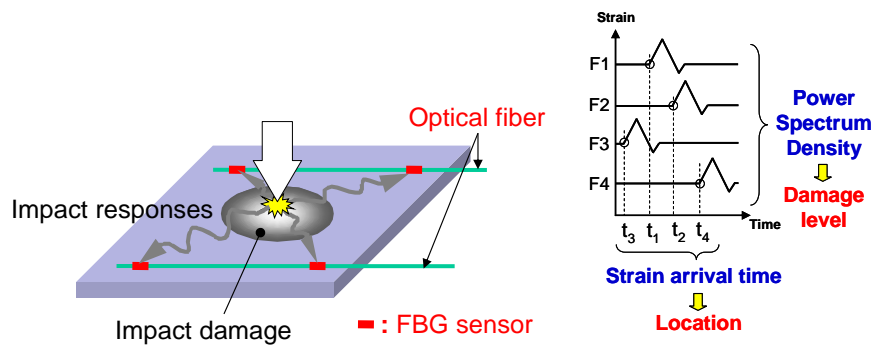


Fig. 30 Measured and calculated strain distribution in the adhesive layer of CFRP foam-core sandwich structures



(a) Optical Intensity measurement method



(b) Strain measurement method with multiple FBG sensors

Fig. 31 Impact Damage Detection Method

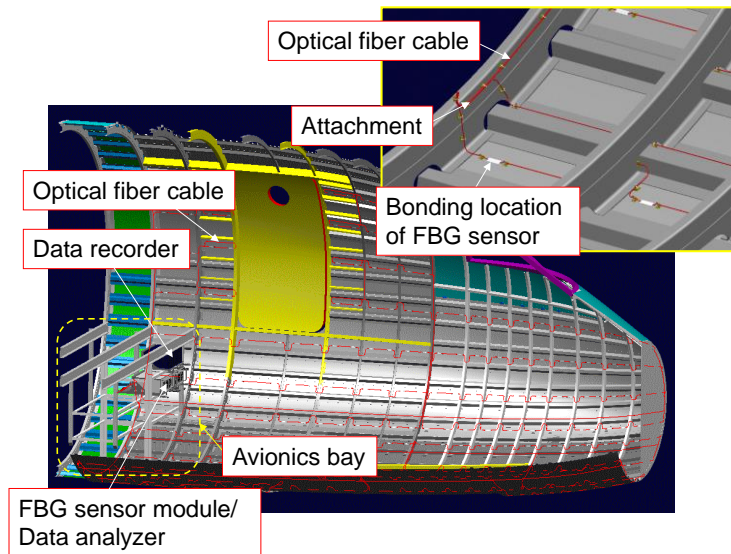
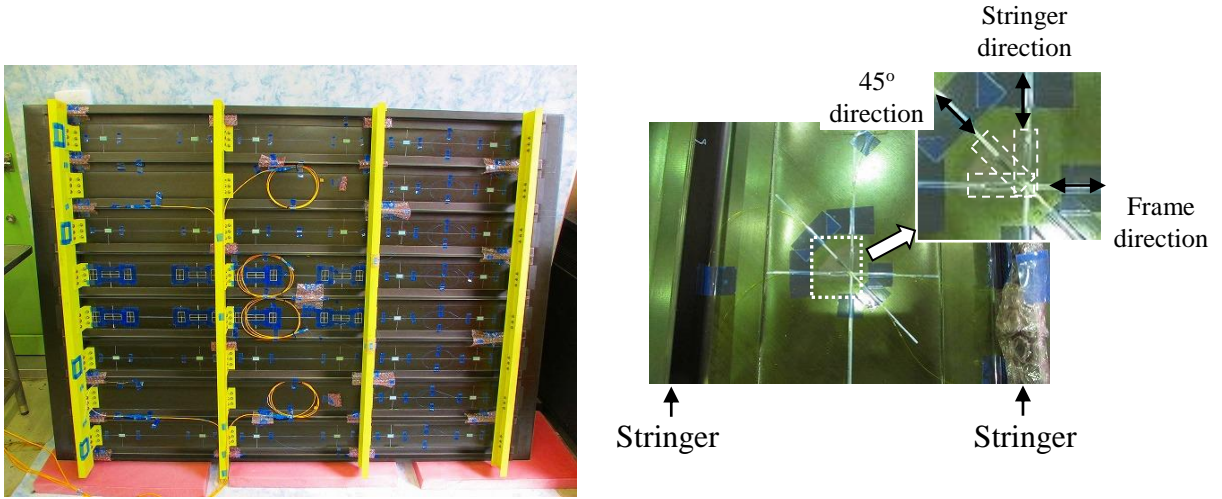


Fig. 32 Typical sensor installation



(a)CFRP stiffened panel
(Looking from stringer side)

□□□□ : FBG sensor
(b)Sensor arrangement

Fig. 33 Sensor arrangement of CFRP stiffened panel for impact test

		<p>FBG optical fiber sensor :</p> <ul style="list-style-type: none"> ➢ Detector of the Lamb wave. ➢ It can measure wide frequency range of the wave. ➢ It's bonded on the surface of the structure. <p>MFC piezoelectric actuator :</p> <ul style="list-style-type: none"> ➢ Source of the Lamb wave. ➢ It can oscillate the wave with high directionality. ➢ It's bonded on the surface of the structure.
--	--	--

Fig. 34 Overview of the SHM system.

<p>Schematics of the test specimen</p>	<p>➢ Disbond was grown gradually from the top of the repair patch with 4 times insertion of a scraper.</p> <p>Diagnosis results with SHM system</p> <p>Diagnosis results with conventional NDT</p>
--	--

Fig. 35 Schematics of the test specimen and Diagnosis results.

Table 2 Comparison table of LEF

$N_T: x N_0^*$	Non-Pa ^{**} : Eqn.(2)	Pa ^{**} : Eqn.(2)	CMH-17 ^{***} :Eqn.(1)
1	1.29	1.35	1.18
2	1.20	1.23	1.13
3	1.15	1.17	1.10
5	1.09	1.11	1.06
10	1.03	1.03	1.02
13.3	1	1	1

* N_0 : Design life

** Pa : parametric, Non-Pa: Non parametric

*** $(\alpha_L, \alpha_r)_{mode} = (1.25, 20.0)$

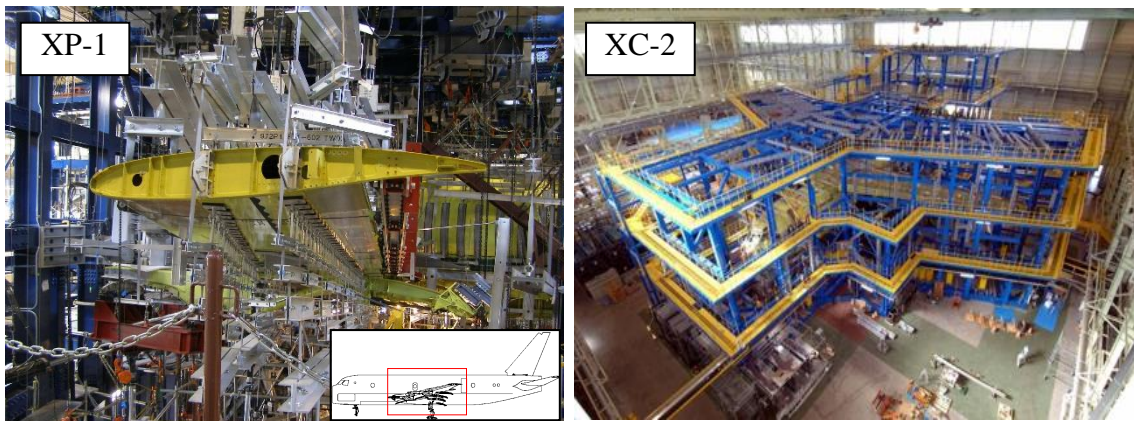


Fig. 36 Strength Test of XP-1 and XC-2 (Ministry of Defense, Japan)



Fig. 37 Strength Test of ATD (Ministry of Defense, Japan)

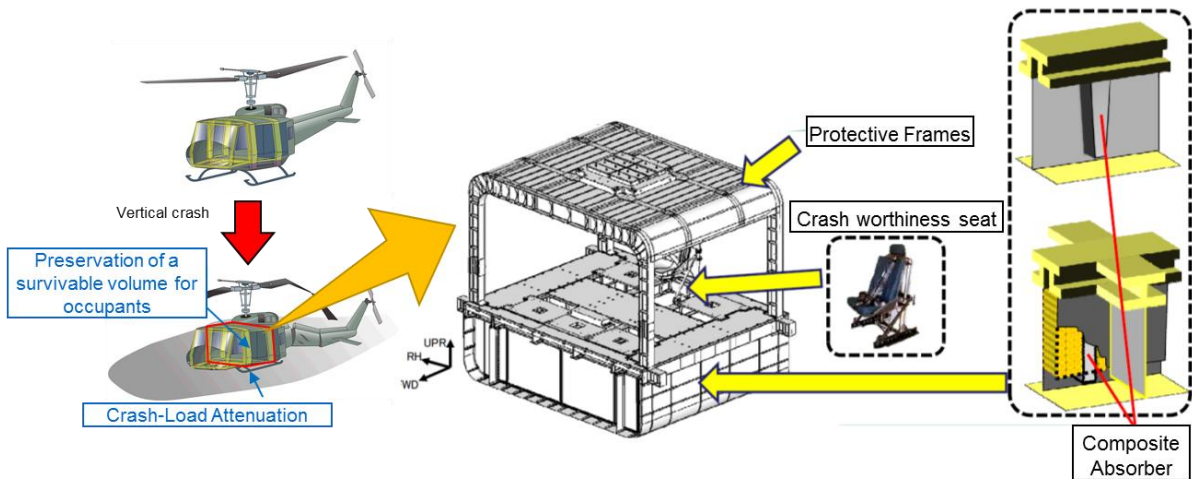


Fig. 38 Helicopter cabin-component with composite absorbers (Ministry of Defense, Japan)



Fig. 39 Curved Panel Fatigue Test Fixture for MRJ200

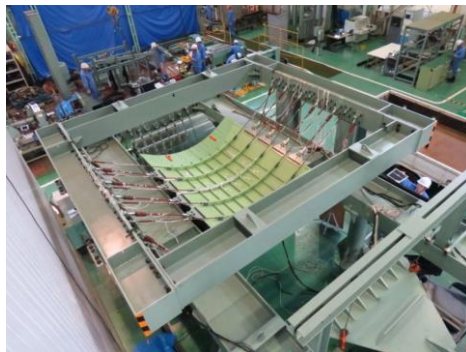


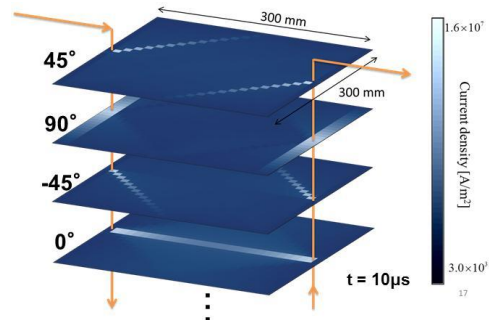
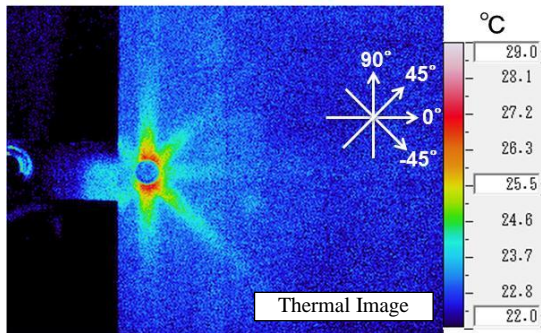
Fig. 40 Curved Panel on Test Fixture



Fig. 41 US-2

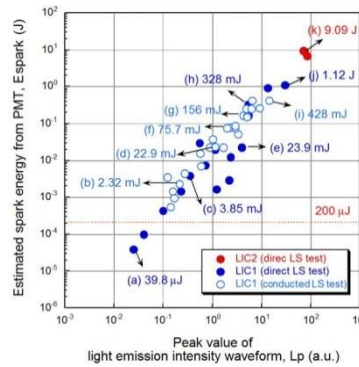
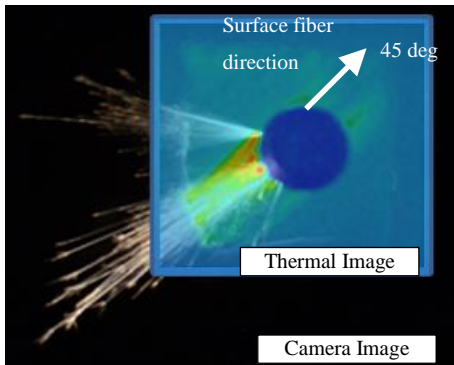


Fig. 42 Image of US-2 Firefighting Amphibian



Anisotropy of Current Density by Test Current Density Simulation of CFRP Layers

Fig. 43 Tri-Prism FDTD Method



Spark from the fastener head Correlation of spark light intensity and energy

Fig. 44 Spark Ignition Energy Estimation